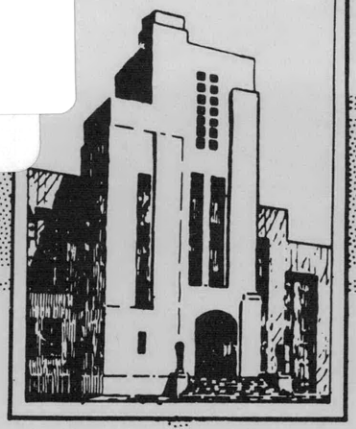

DEPARTMENT OF THE NAVY

DAVID TAYLOR MODEL BASIN

HYDROMECHANICS

AERODYNAMICS

STRUCTURAL MECHANICS

APPLIED MATHEMATICS

INVESTIGATIONS OF VIBRATORY FORCES INDUCED BY PROPELLERS

(Untersuchungen über die Vibrationserregenden Kräfte am Propeller)

by

Dipl. Phys. J. Krohn

Translated by W.B. Hinterthan

February 1962

Translation 303

INVESTIGATIONS OF VIBRATORY FORCES INDUCED BY PROPELLERS*

(Untersuchungen über die Vibrationserregenden Kräfte am Propeller)

by

Dipl. Phys. J. Krohn

I. Krohn, J., "THE MEASURING METHOD, THE CALCULATION, AND THE CONSTRUCTION OF THE MEASURING ELEMENTS," HSVA Report 1120 (Mar 1957).

II. Krohn, J., "TEST PROCEDURE AND RESULTS," HSVA Report 1121 (May 1957).

III. Krohn, J., "EXPANSION OF THE INSTRUMENTATION TO MEASURE THRUST FLUCTUATION," HSVA Report 1148 (Jan 1958).

Translated by W.B. Hinterthan

February 1962 Translation 303

*Resumé of HSVA Reports 1120, 1121, 1148, and HSVA Publication 302.

TABLE OF CONTENTS

ABSTRACT

A method for and the construction of an instrument to measure thrust fluctuations and torque oscillations on a propeller working behind a ship model are given. The propeller shaft is constructed as a hollow shaft in which a second shaft, the measuring shaft, is mounted. The twist of this measuring shaft is transformed by a condenser into an electrical alternating voltage fed by a frequency generator. The modulated alternate voltage is fed into an amplifier connected to a recording instrument. The thrust-measuring instrument is added to the torque-measuring device. The deformation of a diaphragm, caused by the thrust, is measured by an inductive pickup system.

Calculations are given to determine the electrical and mechanical dimensions of the instruments. Results of tests conducted with 3-, 4-, and 5-bladed propellers are given.

I. THE MEASURING METHOD, THE CALCULATION, AND THE CONSTRUCTION OF THE MEASURING ELEMENTS

A. INTRODUCTION

The torsional oscillations in the shafts of ships are excited partly by the engines and partly by hydrodynamic forces acting on the propeller. The oscillations induced by the engines can be calculated, but the hydrodynamic forces acting on the propeller are difficult to determine by calculation because they are so manifold. A means to determine the torsional oscillations on the propeller is by model tests. A new measuring device had to be developed since the existing instruments are not able to measure the oscillations continuously. Thus, this device should record the oscillation, should have a very high natural frequency, and should be free of foreign influences, especially those caused by friction in the bearings. The use of electronic instrumentation makes the recording of the measured values possible. It is desirable to establish the natural frequency of the instrument above the anticipated measured frequencies and in addition limit the highest measured frequency to 80 percent of the natural. If this requirement is not met, there is danger of resonance effects which would give misleading results, and it would be necessary to find a correction function by dynamic calibration. This correction function, in general, is in the vicinity of the resonance peak and depends very much on the damping. The damping itself changes with the harmonics and the existing hydrodynamic condition; therefore, it is very difficult, if not impractical, to determine the correction function by calibration. It is necessary for the bearing to be free from friction influences because the shaft friction torques are transferred to the measuring devices, which are then superimposed on those torques caused by the propeller, and thus the measuring devices give misleading results. In general, the measured torque is larger than the real torque caused by the propeller. On the other hand, oscillations are amplified by this friction which changes the real measured

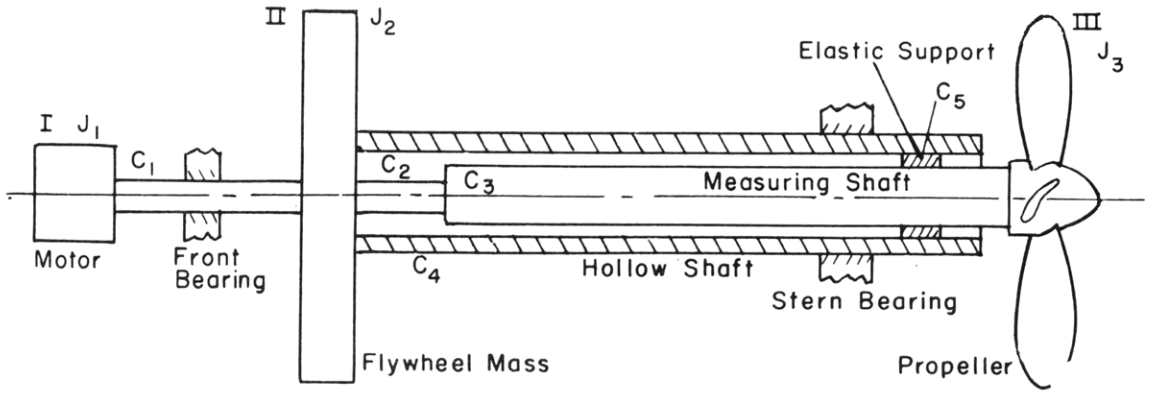

Figure 1

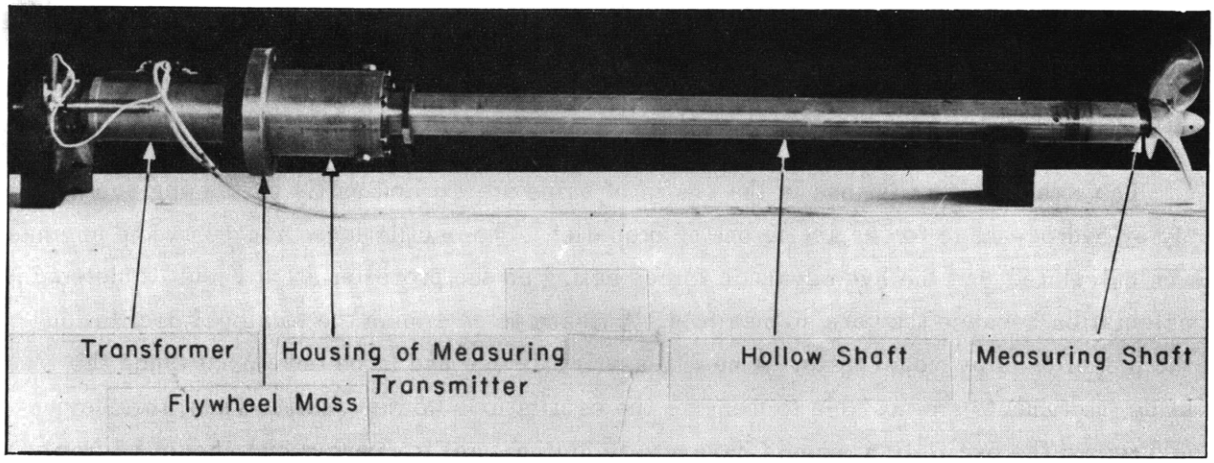

Figure 2

values in regard to the amplitude and frequency. Therefore, it is necessary that the devices between the propeller and the measured values are nct influenced by bearing disturbances. To satisfy all these conditions (bearing friction and high natural frequency), the instrument shown in Figure 1 was designed. The propeller is fastened to a "measuring shaft" which extends to a flywheel mass by means of an intermediate shaft of smaller diameter. The twist angle of the smaller shaft is indicated by an electronic device. A hollow shaft is pushed over the measuring shaft and is rigidly connected to the flywheel mass. At the end where the propeller is located the hollow shaft is supported by the stern bearing. A torsional elastic support is installed at this end between the measuring shaft and the hollow shaft. At the other end of the flywheel mass the shaft is supported by a front bearing. The drive motor is coupled to this blunt shaft.

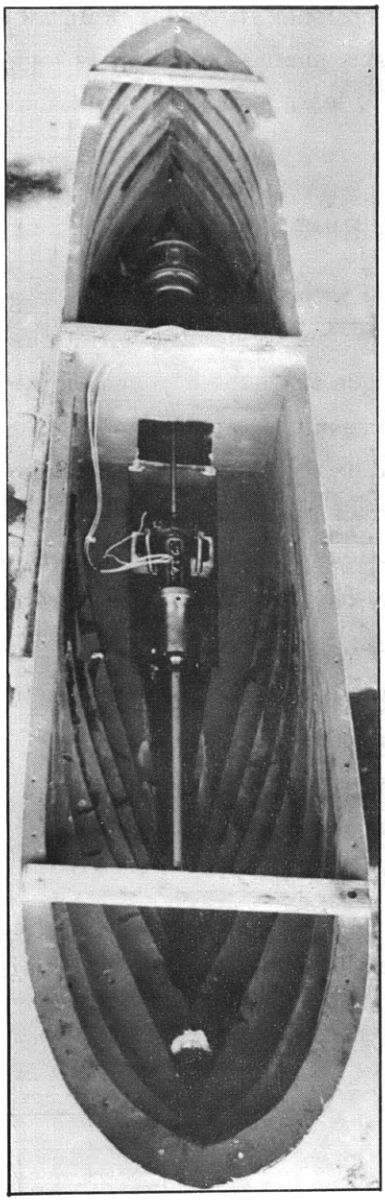

The transmitter of the measured values is attached to the measuring shaft and is located at the left side of the flywheel mass. It transmits the measured values from the rotating shaft to the amplifier recording system. Figure 2 shows the transmitter housing, and Figures 3 and 4 show the instrument installed on the model. The whole measuring system forms an oscillating system. When choosing the flywheel mass correctly, we ascertain that the whole system, in regard to its oscillation, decomposes into two-part systems, e.g., it uncouples.

Thus, all disturbances which result from the driving side and the front bearing are eliminated during the measurements. Also, torques caused by the friction of the stern bearings

Figure 3

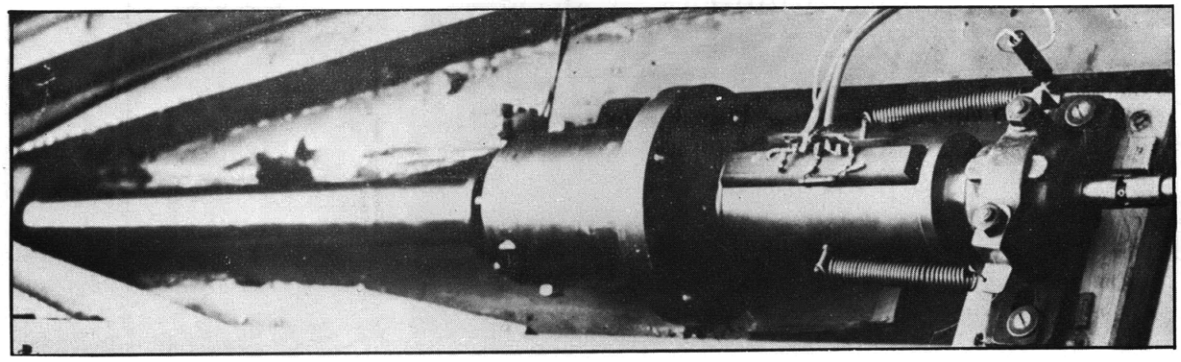

Figure 4

become ineffective if the flywheel mass has a sufficient torsional stiffness. We must also consider that the natural frequency of the system—measuring shaft + propeller—is high enough. Calculations of the mechanical systems were carried out to learn about the dimensions of the construction elements.

B. THE CALCULATIONS OF THE MECHANICAL MEASURING SYSTEM

The system "motor-flywheel-propeller" is connected with the restoring moments C_1, C_2, and C_3 by three coupling members. This system carries out torsional oscillations as a result of the elastic coupling. A periodical additional torque m_1, superimposed on the average torque, acts on the anchor of the motor when rotating as a result of the change of the poles. In the same manner an additional torque m_3, superimposed on the average torque, acts on the propeller. This torque is periodic and is caused as the blades pass the stern. Also, a moment m_4 acts on the hollow shaft as a result of the bearing friction. The restoring moment of the hollow shaft is C_4. This torsional oscillation system may be substituted by a longitudinal oscillation system. The following correspondence is valid:

Moment of inertia	←- - - -→	Mass
Outer moment	←- - - -→	Outer force
Restoring moment	←- - - -→	Restoring force
Angle deflection	←- - - -→	Linear deflection

The "ersatz" system of masses and springs is given in Figure 5.

The inner damping of this system is negligible. The damping becomes significant to the natural frequency at higher values.* The force equilibrium for the system consisting of masses, and springs is

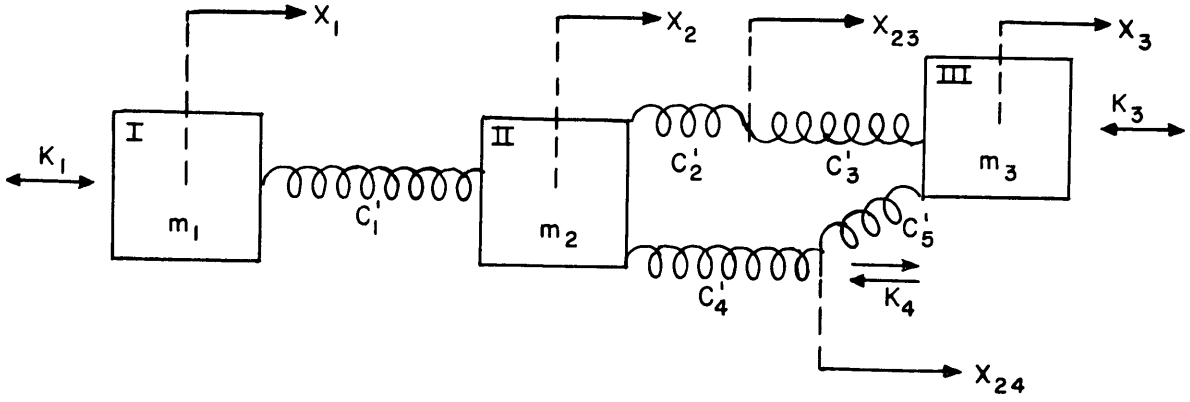

Figure 5

*Den Hartog and Mesmer, "Mechanical Oscillation" (Mechanische Schwingungen), Second Edition, Paragraph 74.

$$m_1\ddot{x}_1 = -C_1'(x_1 - x_2) + K_1$$

$$m_2\ddot{x}_2 = C_1'(x_1 - x_2) - C_2'(x_2 - x_{23}) - C_4'(x_2 - x_{24})$$

$$m_3\ddot{x}_3 = C_3'(x_{23} - x_3) + K_3$$

$$0 = C_2'(x_2 - x_{23}) - C_3'(x_{23} - x_3)$$

$$0 = C_4'(x_2 - x_{24}) + K_4$$

Here the restoring force of the elastic support is neglected because of the small spring constant. Correspondingly, we obtain for the torque-equilibrium of the torsional system, the following equations, if ϕ_{23} and ϕ_{24} will be eliminated by means of the two last equations.

$$\begin{aligned} J_1\ddot{\phi}_1 + C_1\phi_1 - C_1\phi_2 &= M_1 \\ J_2\ddot{\phi}_2 - C_1\phi_1 + (C_1 + \epsilon)\phi_2 - \epsilon\phi_3 &= M_4 \\ J_3\ddot{\phi}_3 - \epsilon\phi_2 + \epsilon\phi_3 &= M_3 \end{aligned} \qquad [1]$$

where $\epsilon = \dfrac{C_2 C_3}{C_2 + C_3}$.

First, the natural frequency of the system has to be determined. This is obtained if Equations [1] are homogeneous and if $M_1 = M_3 = M_4 = 0$. With the expression $\phi_\nu = \Phi_\nu \cdot \sin \bar{\omega} t$ we obtain

$$\begin{aligned} -J_1\bar{\omega}^2\Phi_1 + C_1\Phi_1 - C_1\Phi_2 &= 0 \\ -J_2\bar{\omega}^2\Phi_2 - C_1\Phi_1 + (C_1 + \epsilon)\Phi_2 - \epsilon\Phi_3 &= 0 \\ -J_3\bar{\omega}^2\Phi_3 - \epsilon\Phi_2 + \epsilon\Phi_3 &= 0 \end{aligned}$$

as the equation system for determination of the three unknown amplitudes. This equation system will not have a trivial solution if the following holds true:

$$\begin{vmatrix} C_1 - J_1\bar{\omega}^2 & -C_1 & 0 \\ -C_1 & C_1 + \epsilon - J_2\bar{\omega}^2 & -\epsilon \\ 0 & -\epsilon & \epsilon - J_3\bar{\omega}^2 \end{vmatrix} = 0$$

From this is derived:

$$\bar{\omega}^2 \{ J_1 J_2 J_3 \bar{\omega}^4 - [C_1 J_3 (J_1 + J_2) + \epsilon J_1 (J_2 + J_3)] \bar{\omega}^2 + C_1 \epsilon (J_1 + J_2 + J_3) \} = 0$$

After the solution of $\bar{\omega}^2$, C_1, or ϵ, we find:

$$\bar{\omega}_2^2 = 0$$

$$\bar{\omega}_{1,3}^2 = \frac{1}{2}\left\{\frac{C_1+\epsilon}{J_2} + \frac{C_1}{J_1} + \frac{\epsilon}{J_3} \pm \sqrt{\left(\frac{C_1-\epsilon}{J_2} + \frac{C_1}{J_1} - \frac{\epsilon}{J_3}\right)^2 + 4\frac{C_1\epsilon}{J_2^2}}\right\}$$

$$\epsilon = J_3\,\bar{\omega}_3^2 \cdot \frac{C_1\left(\frac{1}{J_1}+\frac{1}{J_2}\right) - \bar{\omega}_3^2}{C_1\left(\frac{1}{J_1}+\frac{1}{J_2}+\frac{J_3}{J_1 J_2}\right) - \bar{\omega}_3^2\left(1+\frac{J_3}{J_2}\right)}$$

$$C_1 = J_1\,\bar{\omega}_1^2 \cdot \frac{\epsilon\left(\frac{1}{J_3}+\frac{1}{J_2}\right) - \bar{\omega}_2^2}{\epsilon\left(\frac{1}{J_3}+\frac{1}{J_2}+\frac{J_1}{J_2 J_3}\right) - \bar{\omega}_2^2\left(1+\frac{J_1}{J_2}\right)}$$

If $J_1 << J_2$ and $J_3 << J_2$, ϵ becomes

$$\epsilon = J_3\,\bar{\omega}_3^2$$
$$C_1 = J_1\,\bar{\omega}_1^2 \qquad [2]$$

This means that the oscillation system uncouples and breaks down into two-part systems which oscilliate independently of one another.

We now have to investigate how far the system really uncouples. Three moments of inertia are calculated for this purpose:

1. Motor (standard type used at HSVA):
   Diameter of armature = 100 mm
   Length of armature = 100 mm
   $J_1 = \frac{\pi}{2}\frac{\gamma}{g} \cdot L \cdot r^4$
2. Propeller:
   Diameter = 0.2 m
   $Fa/F = 0.45$ $\qquad \gamma = 7600$ kg/m^3
   $d_i/D = 0.048$ $\qquad J_3 = \frac{(G\,D^2)}{4\,g}$
   $d_u/D = 0.0037$ $\qquad (G\,D^2) = 0.00396$ kg·m^2

Here the flywheel mass is given by

$$(GD^2) = C_1 \cdot C_2 \cdot C_3 \cdot C_4 \cdot \gamma \cdot \frac{Fa}{F} \cdot \frac{d_i}{D} D^5$$

with

$$C_1 = 1.04; \quad C_2 = C_3 = 1; \quad C_4 = 0.15 \left(1 + \frac{d_u}{d_i}\right) - 0.089 = 0.0726$$

3. Flywheel mass:

$$r = 0.1\,\text{m}$$

$$\gamma = 7800\ \text{kg/m}^3$$

$$J_2 = \frac{\pi}{2} \cdot \frac{\gamma}{g} \cdot L \cdot r^4$$

From this we obtain:

Motor: $J_1 = 0.00078$ kg·m·sec^2
Mass: $J_2 = 0.0125$ kg·m·sec^2
Propeller: $J_3 = 0.0001$ kg·m·sec^2

The moment of inertia J_2 is large compared to the moments J_1 and J_3. This means that the system is uncoupled and that the dimensions of the shafts can be calculated by Equations [2].

Now we need to solve the system of the unhomogeneous differential Equations [1]. We put $M_1 = D_1 \sin \omega_1 \cdot t$ and $M_3 = D_3 \sin \omega_3 \cdot t$. Then we obtain

$$J_1 \ddot{\phi}_1 + C_1 \phi_1 - C_1 \phi_2 = D_1 \sin \omega_1 t$$

$$J_2 \ddot{\phi}_2 - C_1 \phi_1 + (C_1 + \epsilon)\, \phi_2 - \epsilon\, \phi_3 = M_4$$

$$J_3 \ddot{\phi}_3 - \epsilon \phi_2 + \epsilon \phi_3 = D_3 \sin \omega_3 t$$

With the assumption that

$$\phi_\nu = \Phi_{\nu 1} \sin \omega_1 t + \Phi_{\nu 3} \sin \omega_3 t + g_\nu(t) \qquad (\nu = 1, 2, 3)$$

we obtain the equations for $\phi_{\nu 1}$ and $\phi_{\nu 2}$:

$$(C_1 - J_1 \omega_1^2)\Phi_{11} - C_1 \Phi_{21} = D_1 \qquad [3a]$$

$$(\epsilon - J_3 \omega_1^2)\Phi_{31} - \epsilon\, \Phi_{21} = 0 \qquad [3b]$$

$$(\alpha - J_2 \omega_1^2)\Phi_{21} - C_1 \Phi_{11} - \epsilon \Phi_{31} = 0 \qquad \alpha = C_1 + \epsilon \qquad [3c]$$

$$(\alpha - J_2 \omega_3^2)\Phi_{23} - C_1 \Phi_{13} - \epsilon \Phi_{33} = 0 \qquad [3d]$$

$$(C_1 - J_1\omega_3^2)\Phi_{13} - C_1\Phi_{23} = 0 \qquad [3e]$$

$$(\epsilon - J_3\omega_3^2)\Phi_{33} - \epsilon\Phi_{23} = D_3 \qquad [3f]$$

and three equations for g_ν

$$J_1\ddot{g}_1 + C_1 g_1 - C_2 g_2 = 0 \qquad [4a]$$

$$J_2\ddot{g}_2 + \alpha g_2 - C_1 g_1 - \epsilon g_3 = M_4 \qquad [4b]$$

$$J_3\ddot{g}_3 + \epsilon g_3 - \epsilon g_2 = 0 \qquad [4c]$$

As shown, Equations [3a] to [3c] are independent of Equations [3d] to [3f]. By reversing indices 1 and 3, the systems will be combined. Then we obtain the following solution:

$$\Phi_{11} = \frac{D_1}{\Lambda_1}\cdot\{(\alpha - J_2\omega_1^2)(\epsilon - J_3\omega_1^2) - \epsilon^2\} \qquad \Phi_{13} = \frac{D_3 C_1 \epsilon}{\Lambda_3}$$

$$\Phi_{21} = \frac{D_1 C_1}{\Lambda_1}(\epsilon - J_3\omega_1^2) \qquad \Phi_{23} = \frac{D_3\epsilon}{\Lambda_3}(C_1 - J_1\omega_3^2)$$

$$\Phi_{31} = \frac{D_1 \epsilon C_1}{\Lambda_1} \qquad \Phi_{33} = \frac{D_3}{\Lambda_3}\cdot\{(\alpha - J_2\omega_3^2)(C_1 - J_1\omega_3^2) - C_1^2\}$$

$$\Lambda_1 = (C_1 - J_1\omega_1^2)(\alpha - J_2\omega_1^2)(\epsilon - J_3\omega_1^2) - C_1^2(\epsilon - J_3\omega_1^2) - \epsilon^2(C_1 - J_1\omega_1^2)$$

$$\Delta_3 = (C_1 - J_1\omega_3^2)(\alpha - J_2\omega_3^2)(\epsilon - J_3\omega_3^2) - C_1^2(\epsilon - J_3\omega_3^2) - \epsilon^2(C_1 - J_1\omega_3^2)$$

Now we have to determine the function g_ν. For this purpose it would be practical to combine the system of three equations into one equation for one of the g_ν. If we assume that g_1 (that is, all derivations of g_1), are known, we will have at first three equations for the four unknowns g_2, $\ddot{g}_2$, g_3, and $\ddot{g}_3$. Now it is necessary to look for further equations. This is possible by differentiation of the existing equations:

$$J_1\ddot{g}_1 + C_1 g_1 - C_1 g_2 = 0 \qquad [4a]$$

$$J_2\ddot{g}_2 + \alpha g_2 - C_1 g_1 - \epsilon g_3 = M_4 \qquad [4b]$$

$$J_3\ddot{g}_3 + \epsilon g_3 - \epsilon g_2 = 0 \qquad [4c]$$

$$J_2 \ddddot{g}_2 + \alpha \ddot{g}_2 - C_1 \ddot{g}_1 - \epsilon \ddot{g}_3 = \ddot{M}_4 \quad \left[\frac{d^2}{dt^2}\ (b)\right] \qquad [4d]$$

$$J_1 \ddddot{g}_1 + C_1 \ddot{g}_1 - C_1 \ddot{g}_2 = 0 \quad \left[\frac{d^2}{dt^2}\ (a)\right] \qquad [4e]$$

$$J_1 \dddddot{g}_1 + C_1 \ddddot{g}_1 - C_1 \ddddot{g}_2 = 0 \quad \left[\frac{d^4}{dt^4}\ (a)\right] \qquad [4f]$$

By means of the first five equations we are able to determine the five unknowns g_2, $\ddot{g}_2$, $\ddddot{g}_2$, g_3, and $\ddot{g}_3$ in relation to g_1, $\ddot{g}_1$, and $\ddddot{g}_1$. By substituting $\ddddot{g}_2$ in Equation [4f], we obtain the equation for g_1. By exchanging indices 1 and 3, [4a] transforms into [4c] and vice versa. Now we have:

$$x_1 = g_2; \quad x_2 = \ddot{g}_2; \quad x_3 = \ddddot{g}_2; \quad x_4 = g_3; \quad x_5 = \ddot{g}_3$$

and

$$x_1 = \frac{J_1}{C_1} \ddot{g}_1 + g_1 \qquad [5a]$$

$$\alpha x_1 + J_2 x_2 - \epsilon x_4 = M_4 + C_1 g_1 \qquad [5b]$$

$$\epsilon x_1 - \epsilon x_4 - J_3 x_5 = 0 \qquad [5c]$$

$$\alpha x_2 + J_2 x_3 - \epsilon x_5 = \ddot{M}_4 + C_1 \ddot{g}_1 \qquad [5d]$$

$$x_2 = \frac{J_1}{C_1} \ddddot{g}_1 + \ddot{g}_1 \qquad [5e]$$

$$J_1 \dddddot{g}_1 + C_1 \ddddot{g}_1 - C_1 x_3 = 0 \qquad [5f]$$

The solutions of Equations [5a] through [5e] are:

$$x_1 = \frac{J_1}{C_1} \ddot{g}_1 + g_1$$

$$x_2 = \frac{J_1}{C_1} \ddddot{g}_1 + \ddot{g}_1$$

$$x_3 = -\frac{J_1}{C_1}\left(\frac{\epsilon}{J_3} + \frac{\alpha}{J_2}\right)\ddddot{g}_1 - \epsilon\left(\frac{1}{J_2} + \frac{1}{J_3} + \frac{J_1}{J_2 J_3}\right)\ddot{g}_1 + \frac{\ddot{M}_4}{J_2} + \frac{\epsilon}{J_3} \cdot \frac{M_4}{J_2}$$

$$x_4 = \frac{J_1 J_2}{C_1 \epsilon} \dddot{g}_1 + \frac{1}{\epsilon}\left(J_2 + \frac{\alpha}{C_1} J_1\right) \ddot{g}_1 + \frac{1}{\epsilon}(\alpha - C_1)\, g_1 - \frac{M_4}{\epsilon}$$

$$x_5 = -\frac{J_1 J_2}{C_1 J_3} \dddot{g}_1 - \frac{J_1 + J_2}{J_3} \ddot{g}_1 + \frac{M_4}{J_3}$$

Thus we obtain:

$$J_1 \dddot{f}_1 + J_1\left(\frac{C_1}{J_1} + \frac{\epsilon}{J_3} + \frac{\alpha}{J_2}\right)\ddot{f} + C_1 \epsilon \left(\frac{1}{J_2} + \frac{1}{J_3} + \frac{J_1}{J_2 J_3}\right) f_1 = \frac{C_1}{J_2} \ddot{M}_4 + \frac{C_1 \epsilon}{J_3 J_2} M_4$$

where $f_1 = \ddot{g}_1$. For the moment M_4 we write

$$M_4 = \sum_{\mu} M_{4\mu} \cdot e^{-\beta_\mu |t - t_\mu|}$$

(See Figure 6.)

This function is in the vicinity of $t = t_\mu$ different from zero but otherwise practically equal to zero so that M_4 is a moment existing at any time t_μ; otherwise it disappears. In the same way we can substitute M_4 for a δ function. With the expression

$$f_1 = \sum_{\mu} f_{1\mu} \cdot e^{-\beta_\mu |t - t_\mu|}$$

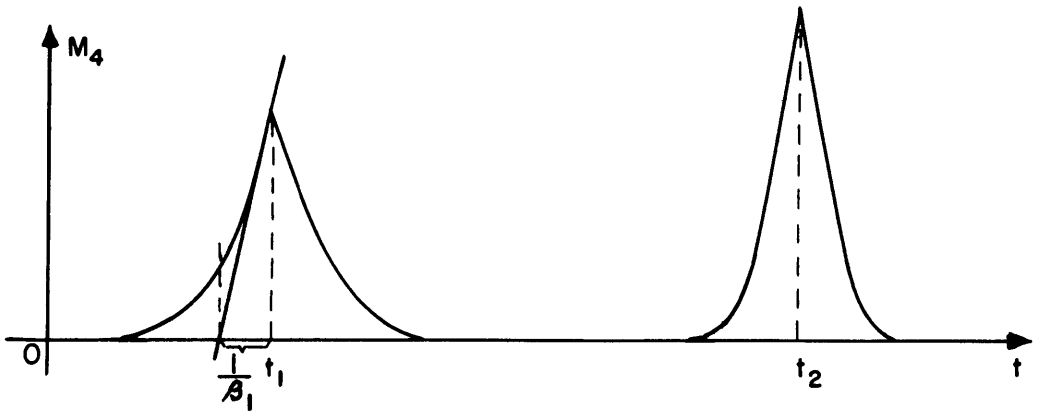

Figure 6

we obtain

$$J_1 \cdot \left\{ \beta_\mu^4 + \left(\frac{C_1}{J_1} + \frac{\epsilon}{J_3} + \frac{\alpha}{J_2} \right) \beta_\mu^2 + C_1 \epsilon \left(\frac{1}{J_1 J_2} + \frac{1}{J_1 J_3} + \frac{1}{J_2 J_3} \right) \right\} \cdot f_{1\mu}$$

$$= \left(\frac{C_1}{J_2} \cdot \beta_\mu^2 + \frac{C_1 \epsilon}{J_3 J_2} \right) M_{4\mu}$$

With the abbreviation

$$\Delta_\mu^* = \beta_\mu^4 + \left(\frac{C_1}{J_1} + \frac{\epsilon}{J_3} + \frac{\alpha}{J_2} \right) \beta_\mu^2 + C_1 \epsilon \left(\frac{1}{J_1 J_2} + \frac{1}{J_2 J_3} + \frac{1}{J_3 J_1} \right)$$

$f_{1\mu}$ becomes

$$f_{1\mu} = \frac{M_{4\mu}}{\Delta_\mu^*} \cdot \frac{C_1}{J_2 J_1} \cdot \left(\beta_\mu^2 + \frac{\epsilon}{J_3} \right)$$

We obtain corresponding expressions for the values $f_{2\mu}$ and $f_{3\mu}$ so that finally g_1, g_2, and g_3 become

$$g_1 = \sum_\mu \frac{M_{4\mu}}{\Delta_\mu^*} \cdot \frac{1}{J_2 \beta_\mu^2} \cdot \frac{C_1}{J_1} \left(\beta_\mu^2 + \frac{\epsilon}{J_3} \right) \cdot e^{-\beta_\mu |t - t_\mu|}$$

$$g_2 = \sum_\mu \frac{M_{4\mu}}{\Delta_\mu^*} \cdot \frac{1}{J_2 \beta_\mu^2} \cdot \left(\beta_\mu^2 + \frac{C_1}{J_1} \right) \left(\beta_\mu^2 + \frac{\epsilon}{J_3} \right) \cdot e^{-\beta_\mu |t - t_\mu|}$$

$$g_3 = \sum_\mu \frac{M_{4\mu}}{\Delta_\mu^*} \cdot \frac{1}{J_2 \beta_\mu^2} \cdot \frac{\epsilon}{J_3} \left(\beta_\mu^2 + \frac{C_1}{J_1} \right) \cdot e^{-\beta_\mu |t - t_\mu|}$$

Now that the general equation of the oscillation system is solved, some remarks for practical use follow. As already shown, $J_1 << J_2$ and $J_3 << J_2$. In regard to the natural frequency, the system breaks up into two-part systems. Furthermore, we wish that the natural frequencies would be larger than those occurring during the measurements and that disturbances coming from the driving side and bearings could be avoided. If we assume the maximum number of revolutions of the shaft to be $n = 20\ \text{sec}^{-1}$ and demand that (in reference to the revolution) the 10th harmonic will be accurately measured, then the natural frequency, in this case, the frequency $\bar{\nu}_3$ as a result of the uncoupled system, has to be larger than 200 cps. Corresponding to the description on page 2, we will deal with the number values

for $\omega_{3max} = 0.8\,\bar{\omega}_3$ and $\omega_{3max} = 0.5\,\bar{\omega}_3$. According to Equation [2], we then obtain:

$\omega_{3max} = 0.5\,\bar{\omega}_3$	$\omega_{3max} = 0.8\,\bar{\omega}_3$
$\epsilon = 6.31 \cdot 10^2$ kgm	$\epsilon = 2.46 \cdot 10^2$ kgm
$l_2 = 1$m	$l_2 = 1$m
$d_2 = 30$ mm $(C_3 = \infty)$	$d_2 = 24$ mm $(C_3 = \infty)$

The following was considered when calculating these numbers: If we plot C_2 against C_3, corresponding to the definition

$$\epsilon = \frac{C_2 \cdot C_3}{C_2 + C_3} = \text{constant}$$

(Figure 7) and consider that $C = \pi/32 \cdot G \cdot d^4/l$, C_3 has to be made large so that the dimensions of the shaft will not become too large. In this case, it means that C_3 approaches infinity. Therefore, if C_3 approaches infinity and corresponds to the condition where l approaches 0, the shaft has to be constructed without a step (see Figure 7). All other combinations of C_2 and C_3 would require that the diameter of the hollow shaft, which surrounds the torsional shaft, be made too large. This would cause difficulty when installing the shaft into the model, since the stern-boss would have a very large diameter (this diameter would amount to about 40 mm on a 5-m model).

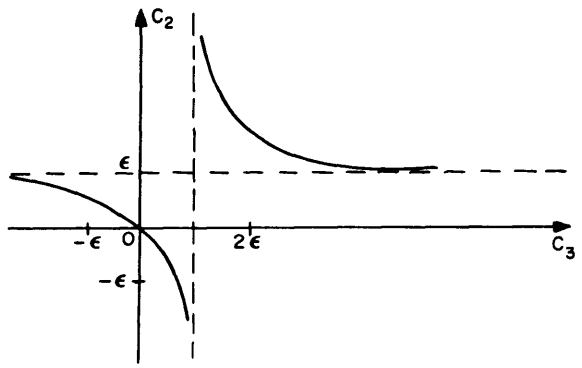

Figure 7

To eliminate disturbances caused at the driving side, it is necessary to manufacture a very soft shaft between the motor and flywheel mass in regard to torsion. This, naturally, goes only so far that the maximum required power can be transmitted. That means that C_1, and thus, according to Equation [2], $\bar{\omega}_1$ have to be so small that the dimensions of this shaft guarantee the transfer of power but not the transfer of any disturbances to the measuring member. Shafts with a diameter of 10 mm (0.394 in.) are used when testing standard models. If the length of the shaft between motor and flywheel mass is 0.5 m, then according to Equation [2] the natural frequency becomes $\bar{\nu}_1 = 32.5$ cps. Furthermore, the armatures of the motors have about 48 poles so that at a revolution of $n = 10$ sec^{-1}, the disturbance frequency, which occurs with pole changes, amounts to 480 cps in this case. This means that $\bar{\omega}_1 << \omega_1$ in the region of the revolutions mainly used. On the other hand, ω_1 and $\bar{\omega}_3$ are of about the same magnitude. Thus, we obtain for the amplitudes caused on the driving side:

$$\Phi_{11} = -\frac{D_1}{J_1 \omega_1^2}$$

$$\Phi_{21} = \frac{\bar{\omega}_1^2}{\omega_1^2} \cdot \frac{D_1(\bar{\omega}_3^2 - \omega_1^2)}{J_2 \left[\omega_1^2 (\bar{\omega}_3^2 - \omega_1^2) + \frac{J_3}{J_2} \bar{\omega}_3^4\right]}$$

$$\Phi_{31} = \frac{\bar{\omega}_1^2}{\omega_1^2} \cdot \frac{D_1 \cdot \bar{\omega}_3^2}{J_2 \left[\omega_1^2 (\bar{\omega}_3^2 - \omega_1^2) + \frac{J_3}{J_2} \cdot \bar{\omega}_3^4\right]}$$

We see that Φ_{21}/Φ_{11} or Φ_{31}/Φ_{11} are in linear ratio to $\bar{\omega}_1^2/\omega_1^2 \cdot J_1/J_2$. Employing these number values, we obtain $\Phi_{21}/\Phi_{11} \approx \Phi_{31}/\Phi_{11} \approx 3.1 \cdot 10^{-4}$, which means that the disturbing amplitudes are relatively small referred to the exciting amplitude. Referred to the amplitude to be measured, Φ_{33} becomes Φ_{21}/Φ_{33} or Φ_{31}/Φ_{33}, respectively, in general, equal to $\bar{\omega}_1^2/\omega_1^2 \cdot D_1/D_3$. It is no mistake to assume that $D_1/D_3 \leqq 1$ because D_1 decreases with an increasing number of revolutions. If this is the case, then $\Phi_{21}/\Phi_{33} \approx \Phi_{31}/\Phi_{33} \approx 5 \cdot 10^{-3}$. Even here the disturbances remain relatively small.

The disturbances caused by the bearing friction can be made arbitrarily small, corresponding to the construction. Essential in this case is the member $M_4/J_2\beta^2$. The times of impact are of the magnitude of 10^{-2} sec; thus $\beta_\mu \approx 10^2$ sec^{-1}. Then it follows that $J_2\beta^2 = 12.5$ kgm. $M_{4\mu}$ is of the magnitude of 10^{-2} kgm as former measurements show, so that $M_4/J_2\beta^2 \approx 10^{-4}$.

As has been shown, it is possible to build a measuring member that corresponds to the dimensions given in the discussion and where frequency is below the natural frequency and is nearly free of disturbances.

C. TWIST MEASUREMENTS OF THE TORSION SHAFT

The twist of the torsion shaft as a result of the applied moments is measured electrically. Existing measuring instruments are used (amplifier with carrier-frequency generator). It was determined that a fitted transmitter is essential, and a "variable" condenser was chosen for this purpose. Principally, inductive transmitter or tension strips (strain gages) can be used, but in this case the use of a condenser seems to be the best method constructionally. The measuring method is based on a change of capacitance caused by voltage changes.

This condenser is built with one of its plates connected to the torsion shaft in such a way that one plate edge is toward the radial direction and the other edge the axial direction.

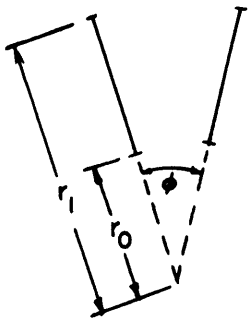

Figure 8

Opposite to this plate is a second plate with its connection shifted in axial direction in reference to the first plate. This condenser is an angle condenser, which means that the opening angle between the plates is changed when twisted. Its capacitance is given by

$$C = \frac{2\pi \epsilon_0 l}{\phi} \cdot \ln \frac{r_1}{r_0}$$

where l is the length of the plate in axial direction,

ϕ is the opening angle, and

r_1 and r_0 are radii that correspond to Figure 8.

When twisted, ϕ changes so that

$$\phi = \phi_0 + \phi_1 + \phi_2 \cdot e^{i\omega t}$$

where ϕ_0 is the angle at rest,

ϕ_1 is the twist angle as a result of a statical moment, and

$\phi_2 \cdot e^{i\omega t}$ is the twist angle as a result of an alternating moment.

If C_0 is defined as the capacitance at rest, namely,

$$C_0 = \frac{2\pi \epsilon_0 l}{\phi_0} \cdot \ln \frac{r_1}{r_0}$$

so is

$$\frac{1}{C} = \frac{1}{C_0} \cdot \left(1 + \frac{\phi_1}{\phi_0} + \frac{\phi_2}{\phi_0} \cdot e^{i\omega t}\right)$$

We notice that if the measuring system fits we are able to measure the static as well as the alternating torque.

A transmitting circuit current corresponding to Figure 9 is connected to the exit of an HF generator having a voltage of $U = U_0 \cdot e^{i\omega_0 t}$ (phases are included in U_0). The alternating capacitance is defined as C (Figure 9), and C_2 defines two additional coupling capacitances which can be built so that they work without disturbances. R_0 defines a resistance to couple the measuring amplifier, and C_B is the blind-capacitance of the feeding cable (cable protection).

Figure 9

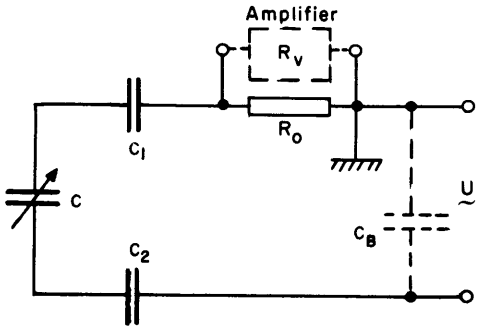

When neglecting C_B, we obtain the following circuit relations

$$U = U_C + U_1 + U_2 + U_{R0}$$

$$\int I\,dt = CU_C = C_1 U_1 = C_2 U_2 = Q$$

$$U_{R0} = R_0 \cdot \frac{I}{1+\alpha}$$

where $\alpha = \dfrac{R_0}{R_v}$ and R_v represents the resistance of the amplifier. Thus we obtain

$$\dot{Q} + \frac{1+\alpha}{R_0} \cdot \left(\frac{1}{C_1} + \frac{1}{C_2} + \frac{1}{C}\right) Q = \frac{1+\alpha}{R_0} \cdot U$$

Introducing

$$\frac{1+\alpha}{R_0}\left[\frac{1}{C_1} + \frac{1}{C_2} + \frac{1}{C_0}\left(1 + \frac{\phi_1}{\phi_0}\right)\right] = \alpha$$

$$\frac{1+\alpha}{R_0 \cdot C_0} \cdot \frac{\phi_2}{\phi_0} = b$$

$$\frac{1+\alpha}{R_0} \cdot U_0 = I_0$$

we obtain

$$\dot{Q} + (a + b \cdot e^{i\omega t})\, Q = I_0 \cdot e^{i\omega_0 t}$$

With the theme

$$Q(t) = \sum_{n=0}^{\infty} Q_n \cdot e^{i(\omega_0 + n\omega)\, t}$$

we obtain

$$\Sigma\, i(\omega_0 + n\omega) \cdot Q_n \cdot e^{i(\omega_0 + n\omega)t} + a\Sigma\, Q_n \cdot e^{i(\omega_0 + n\omega)t}$$

$$b\Sigma\, Q_n e^{i[\omega_0 + (n+1)\omega]t} = I_0 e^{i\omega_0 t}$$

Here the factor $e^{i\omega_0 t}$ is eliminated. For $n = 0$, we obtain

$$Q_0 = I_0 \cdot \frac{a - i\omega_0}{a^2 + \omega_0^2}$$

The coefficient comparison gives for $n > 0$

$$Q_n = -\frac{a - i(\omega_0 + n\omega)}{a^2 + (\omega_0 + n\omega)^2} \cdot b \cdot Q_{n-1}$$

This equation shows that the amplitudes of the upper oscillations become quadratically small.

The voltage drop of the resistance R_0 is of special interest. We obtain

$$U_{R_0} = \frac{R_0}{1 + \alpha} \cdot \dot{Q}$$

Only the first two coefficients of the coefficients of the series for Q will be used. For these we obtain

$$Q_0 = \frac{U_0 C_r}{1 + \dfrac{\omega_0^2 R_0^2 C_r^2}{(1+\alpha)^2}} - i \cdot \frac{U_0 C_r \cdot \dfrac{\omega_0 R_0 C_r}{(1+\alpha)^2}}{1 + \dfrac{\omega_0^2 R_0^2 C_r^2}{(1+\alpha)^2}}$$

$$Q_1 = U_0 \cdot C_r \cdot \frac{1 - \omega_0(\omega_0 + \omega)\dfrac{R_0^2 C_r^2}{(1+\alpha)^2} - i\,(2\omega_0 + \omega)\dfrac{R_0 C_r}{1+\alpha}}{\left[1 + (\omega_0 + \omega)^2 \dfrac{R_0^2 C_r^2}{(1+\alpha)^2}\right]\left[1 + \dfrac{\omega_0^2 R_0^2 C_r^2}{(1+\alpha)^2}\right]} \cdot \frac{C_r}{C_0} \cdot \frac{\phi_2}{\phi_0}$$

In this case

$$\frac{1}{C_r} = \frac{1}{C_1} + \frac{1}{C_2} + \frac{1}{C_0}\left(1 + \frac{\phi_1}{\phi_0}\right)$$

Thus we obtain for the first two voltage members:

$$U_{R_{0,0}} = U_0 \cdot \frac{1}{1+\alpha} \cdot \frac{\omega_0 R_0 C_r}{\sqrt{1 + \left(\frac{\omega_0 R_0 C_r}{1+\alpha}\right)^2}} \cdot \cos(\omega_0 t + \epsilon)$$

and with

$$\tan \epsilon = \frac{1+\alpha}{\omega_0 R_0 C_r}$$

$$U_{R_{0,1}} = U_0 \cdot \frac{1}{1+\alpha} \cdot \frac{(\omega_0+\omega) R_0 C_r}{\sqrt{\left[1 + (\omega_0+\omega)^2 \frac{R_0^2 C_r^2}{(1+\alpha)^2}\right]\left[1 + \frac{\omega_0^2 R_0^2 C_r^2}{(1+\alpha)^2}\right]}} \cdot \frac{C_r}{C_0} \cdot \frac{\phi_2}{\phi_0} \cdot \cos[(\omega_0+\omega) t + \epsilon]$$

and with

$$\tan \epsilon = \frac{1 - \omega_0(\omega_0+\omega)\frac{R_0^2 C_r^2}{(1+\alpha)^2}}{(2\omega_0+\omega)\frac{R_0 C_r}{1+\alpha}}$$

Only the real parts are considered from the physical point of view. Due to the circuit of HF generators and amplifiers (HSVA V02), the voltage part $U_{R_{0,0}}$ is eliminated by compensation (bridge connection). The real voltage carrying the measuring value is $U_{R_{0,1}}$. Here we see the following: Due to the definition, C_r is smaller than C_0. To make $U_{R_{0,1}}$ as large as possible, C_r must be nearly equal to C_0. That, however, means

(a) $C_1 >> C_0$ and $C_2 >> C_0$

To keep $\tan \epsilon$ small, we have to have

(b) $$\frac{\omega_0 R_0 C_r}{1+\alpha} \approx 1$$

Then we obtain

$$\tan \epsilon \approx - \frac{\omega}{2\omega_0 + \omega}$$

Since $\omega_0 = 4.10^5$ cps and $\omega_{max} = 400$ cps, $\tan \epsilon$ in this case becomes

$$|\tan \epsilon| < 0.5 \cdot 10^{-3}$$

Under the assumption of the fulfillment of condition (b) we obtain

$$U_{R_{0,1}} = U_0 \sqrt{\left(1 + \frac{\omega}{\omega_0}\right)} \cdot \frac{1}{2} \cdot \frac{C_r}{C_0} \cdot \frac{\phi_2}{\phi_0} \cdot \cos [(\omega_0 + \omega)t + \epsilon] \qquad [6]$$

and $\left(\frac{\omega}{\omega_0}\right)^2$ can be neglected. As the calculation indicates, the coupling-capacitance must be large in comparison to the measuring-capacitance in order to obtain the highest voltage drop across R_0. Furthermore, the carrier-frequency has to be large compared to the modulation-frequency in order to keep the amplitude independent of the frequency.

The preceding considerations did not include the blind-capacitance. The blind-capacitance caused by the shielding must not suppress the measured values and, therefore, the measuring-capacitance should not be chosen too small. The blind-capacitance is parallel to the measuring-capacitance so that the largest part of the current runs through the blind circuit if the measuring-capacitance is too small and, thus, is lost for the measurement. The blind-capacitance, measuring-capacitance, and coupling-capacitance have to be tuned mutually, and then the phase conditions have to be fulfilled by means of R_0. If we do not neglect C_B—which means that the calculation is based on the block diagram given in Figure 6, including the hatched member—we notice (if Ig represents the total current) that I has to be

$$I = \frac{Ig}{1 + \sqrt{2 \frac{C_B}{C_r}}}$$

if the fulfillment of condition (b) is assumed. Equation [6] has to be multiplied by

$$\left(1 + \sqrt{2 \frac{C_B}{C_r}}\right)^{-1}$$

The expanded condition (a) thus becomes (c)

$$\text{(c)} \quad C_B << C_0; \quad C_0 << C_1; \quad C_0 << C_2$$

It is not necessary to give a number calculation here since only magnitude relations are defined by the relation (c). As an average, the cable-capacitance amounts to $C_B \sim 100$ pF/m per meter. Since we succeed with 0.5-m cable, the values of C_0 and C_1 are chosen as follows: $C_0 \sim 300$ pF and $C_1 = C_2 \sim 1000$ pF. The magnitudes of C_1 and C_2 are determined approximately by reason of manufacturing as shown in the next section.

D. THE TRANSMISSION FROM THE ROTATING TO THE STATIONARY SYSTEM

Two coupling condensers, C_1 and C_2, have been employed in the calculation in Part C and in Figure 9. This is required since the pickup (measuring condenser) shifts in reference to the transmitter and the amplifier. At first, we considered using sliprings as the transmission elements. Changes in the transmission resistance occur, since the brushes are not pressing uniformly. These changes correspond to a voltage change; that is, there is the danger of an error in the measuring values. Difficulties also might occur when a turning transformer is used as the transmission element (L-C member). Thus, the transmission of the measuring value from the rotating to the resting system is done by condensers; see Figure 10. C_1 and C_2 are coupling-capacitances and C is the measuring-capacitance. The part within the dotted line is rotating while the other part is resting. Since it is possible that a bearing-play exists in the axial direction, the part within the dotted line may shift in the direction of the arrows; see Figure 10. A change in coupling-capacitance will occur, which means there will be an error in the measured value. Therefore, the device must be constructed so that there is no change in capacitance. Such a change does not take place in the block diagram as given in Figure 10. The condensers (plate condenser) consist of two plates, one of which is rotating. For a plate condenser, the following is true:

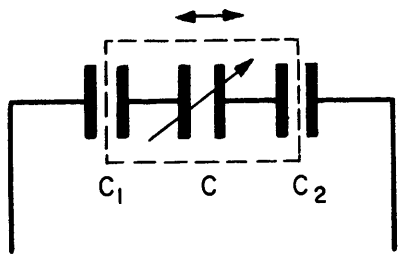

Figure 10

$$\text{(length in meters)}\ \overline{C} = \epsilon_0 \cdot \frac{F}{d}$$

where F is the area of a plate and d is the clearance. Thus, when shifting the axis about Δ, we obtain for C_1, for instance, $d_1 \to d_1 + \Delta$, and for C_2, $d_2 \to d_2 - \Delta$. This means

$$C_1 = \epsilon_0 \cdot \frac{F}{d_1 + \Delta}\ ; \quad C_2 = \epsilon_0 \cdot \frac{F}{d_2 - \Delta}$$

The planes can be built very accurately of identical areas. Since both condensers are in series, $1/C_s$ becomes

$$\frac{1}{C_s} = \frac{1}{C_1} + \frac{1}{C_2} = \frac{1}{\epsilon_0 F} \cdot (d_1 + \Delta + d_2 - \Delta) = \frac{d_1 + d_2}{\epsilon_0 \cdot F}$$

A shift in axial direction is thus balanced, making this system fit as a coupling member. However, C_1 and C_2 cannot be made infinitely large; that means, F is not arbitrarily large and d is not arbitrarily small, since F is limited in upper and lower direction by reasons of practical constructions. However, the calculation of the total circuit indicated that C_s has to be as large as possible. To obtain a large C_s, some condensers have to be connected parallel to one another. A row of plates has to be mounted on the axis behind one another and arranged in a parallel circuit, as shown in Figure 11. C_1 and C_2 each consists of N pairs of plates. When shifting the plates, we obtain

$$C_1 = \epsilon_0 F \frac{N}{d + \Delta}$$

$$C_2 = \epsilon_0 F \frac{N}{d - \Delta}$$

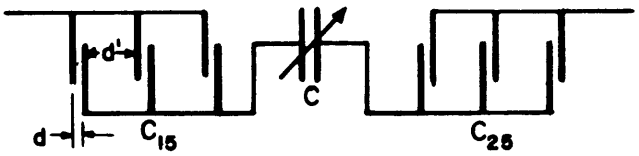

Figure 11

Besides, the plate of one pair forms a condenser with the plate of the other pair, a total each of $N - 1$. Now we obtain

$$C_1' = \epsilon_0 F \frac{N - 1}{d' - \Delta} \qquad C_2' = \epsilon_0 F \frac{N - 1}{d' + \Delta}$$

Consequently;

$$C_{1s} = C_1 + C_1' = \epsilon_0 F \cdot \frac{N \cdot (d' - \Delta) + (N - 1) \cdot (d + \Delta)}{(d + \Delta) \cdot (d' - \Delta)}$$

$$C_{2s} = C_2 + C_2' = \epsilon_0 F \cdot \frac{N \cdot (d' + \Delta) + (N - 1) \cdot (d - \Delta)}{(d - \Delta) \cdot (d' + \Delta)}$$

To obtain an independency from Δ, we require that $\Delta << d'$ and $\Delta << N \cdot d$. Then we obtain

$$C_{1s} = \epsilon_0 \cdot \frac{F}{d + \Delta} \cdot \frac{Nd' + (N-1)\, d}{d'}; \quad C_{2s} = \epsilon_0 \cdot \frac{F}{d - \Delta} \cdot \frac{Nd' + (N-1)\, d}{d'}$$

Consequently, we obtain

$$\frac{1}{C_s} = \frac{1}{C_{1s}} + \frac{1}{C_{2s}} = \frac{1}{\epsilon_0 F} \cdot \frac{d'}{Nd' + (N-1)d} (d + \Delta + d - \Delta)$$

or

$$C_s = \frac{\epsilon_0 F}{2d} \cdot N \cdot \left(1 + \frac{N-1}{N} \frac{d}{d'}\right)$$

From the construction point of view, we try to make $d << d'$. Then

$$C_s = \frac{N}{2} \cdot \frac{\epsilon_0 F}{d}$$

A second possibility in reference to the independence of shifting offers the "cylinder-condenser," the envelope of which surrounds the shaft. For the condenser consisting of two envelopes, we obtain

$$C = 2\pi \cdot \epsilon_0 \cdot \frac{l}{\ln \frac{r_a}{r_1}}$$

where l is the length in meters, and r_1 and r_a are the radii of the inner or outer cylinders, respectively. Introducing $r_a = r_1 + \delta r$ we obtain:

$$C = 2\pi \cdot \epsilon_0 \cdot \frac{l}{\ln \left(1 + \frac{\delta r}{r_1}\right)}$$

l approaches $l + \Delta$ when a shift of Δ takes place. A condenser built according to Figure 12 has the following capacitance (parallel circuit):

$$C = \frac{2\pi \cdot \epsilon_0}{\ln\left(1 + \frac{\delta r}{r_1}\right)} (l + \Delta + l - \Delta)$$

$$= \frac{4\pi \cdot \epsilon_0 \cdot l}{\ln \left(1 + \frac{\delta r}{r_1}\right)}$$

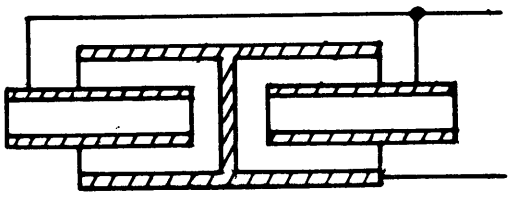

Figure 12

The capacitance of a condenser as given in Figure 12 cannot be chosen arbitrarily from the construction point of view. Therefore, a condenser is composed of several cylinders as shown in Figure 13. The middle parts and the parts shifted from both sides may consist of N cylinders. The capacitance between the nth cylinder of an inserted part and the nth cylinder of the middle part for one side, counting from inward to outward, becomes:

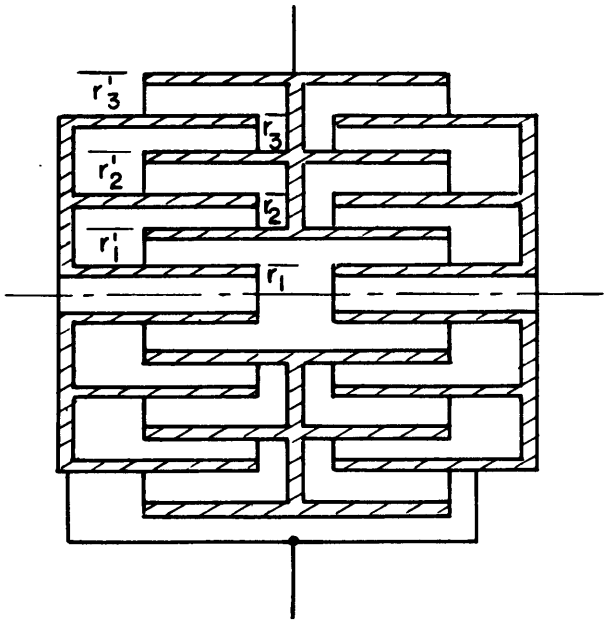

Figure 13

$$C_n = 2\pi \cdot \epsilon_0 \cdot \frac{l}{\ln\left(1+\frac{\delta r}{r_n}\right)}$$

Furthermore, the capacitance between the $(n-1)$th cylinder of an inserted part and the nth cylinder of the middle part becomes for one side:

$$C_n' = 2\pi \cdot \epsilon_0 \frac{l}{\ln\left(1+\frac{\delta r}{r_n'}\right)}$$

We assume the width of the slit δr to be uniform. Now C_n as well as C_n', and also the C_n and the C_n' are located one beneath the other and their sides are parallel to one another. Thus axial shiftings are eliminated and the capacitance of the total condenser becomes

$$C_{1s} = 4\pi \cdot \epsilon_0 \cdot l \cdot \left\{ \sum_{n=1}^{N} \frac{1}{\ln\left(1+\frac{\delta r}{r_n}\right)} + \sum_{n=1}^{N-1} \frac{1}{\ln\left(1+\frac{\delta r}{r_n'}\right)} \right\}$$

We assume that

$$\delta r \ll r_1$$

Then we obtain

$$\ln\left(1+\frac{\delta r}{r_n}\right) = \frac{\delta r}{r_n}$$

and

$$\ln\left(1+\frac{\delta r}{r_n'}\right)=\frac{\delta r}{r_n'}$$

also

$$C_{1s}=4\pi\cdot\overline{\epsilon}_0\frac{l}{\delta r}\left\{\sum_{n=1}^{N}r_n+\sum_{n=1}^{N-1}r_n'\right\}$$

Now all cylinders become the same wall thickness d. Then

$$r_n=r_1+2(n-1)\,(d+\delta r)$$

$$r_n'=r_1'+2(n-1)\cdot(d+\delta r)=r_1+(2n-1)\cdot(d+\delta r)$$

then

$$C_{1s}=4\pi\cdot\epsilon_0\,(2N-1)\cdot\frac{l}{\delta r}\cdot[r_1+(N-1)\cdot(d+\delta r)]$$

Two such condensers are in series, thus:

$$C_s=2\pi\,\epsilon_0(2N-1)\cdot\frac{l}{\delta r}\cdot[r_1+(N-1)\cdot(d+\delta r)]$$

E. CALCULATION OF THE TWO KINDS OF CONSTRUCTION

1. Cylinder Condenser

The radii r_1 and r_N' are determined by the available space of the measuring instrument, and are not variable.

If

r_1 = 17.5 mm d = 1 mm l = 15 mm

r_N' = 71.5 mm r = 1 mm

we obtain:

$$N=14$$

and

$$C_s=981.5\text{ pF}$$

Calculating with a front-plate thickness of 2.5 mm and a width of the slit of 2.5 mm (in axial direction), the length of a condenser becomes 47.5 mm.

2. Plate Condenser

If the radii r_0 and r_1 are given:

$r_0 = 22.5$ mm $\qquad d = 1$ mm

$r_1 = 60$ mm $\qquad N = 20$

we obtain:

$$C_s = 860 \text{ pF}$$

If the plate is assumed to be 2 mm (as a result of the stiffness), and $d' = 5$ mm, then we obtain a length of the condenser of 195 mm.

Since a capacitance C_s of about 1000 pF is required, the cylinder condenser is preferred because of its smaller length (25 percent of the length of the plate condenser). Furthermore, the axial shifting Δ is completely eliminated on the cylindrical condenser whereas it is only approximately eliminated on the plate condenser. Δ/d' would become 0.01 if $\Delta = 0.05$ mm. Calculating with a value of $\phi_2/\phi_0 = 0.8$ for the measuring condenser, a value which is very favorable, the change of the coupling condenser would amount to more than 1 percent in reference to the measuring condenser; that is, the accuracy of the measuring value would amount to 1 percent for this specific reason alone.

II. TEST PROCEDURE AND RESULTS

The model of a trawler was chosen for which the test results with a 3- and 4-bladed propeller were known. The dimensions of the model and the propellers were:

Model			Propeller		
L_{BP}	(m)	3.22	No. of blades	3	4
Beam	(m)	0.56	D (mm)	203	203
Draft	(m)	0.245	P (mm)	228	221
Displacement	(kg)	248.25	P/D	1.117	1.09
C_B		0.562	A_a/A	0.484	0.500

The static calibration was done by attaching a lever arm to the nonrotating measuring shaft. The load was applied by weights. The twist of the shaft causes a deflection of the measuring loop, thus determining the calibration factor (torque per millimeter deflection). The dynamic calibration was done by attaching a device to the rotating shaft, which causes an

alternating torque. This alternating torque is proportional to the square of the shaft revolution, thus a change of the amplitude of the alternating torque is obtained when the revolutions are changed. After the tests the device was statically calibrated for check purposes. The results of these three calibrations are given in Figure 14. The figure indicates the linear working of the transmitter. The calibration gives a calibration factor of 326 gcm/mm deflection.

The test procedure is the same as in a propulsion test. The model is free-moving and driven by the propeller. The measuring device is installed between the motor and the propeller—in this case it is a torsional-vibration instrument. The test is conducted by running at different speeds, each run providing one measuring spot. The torsional vibration is received by the transmitter and the value is fed through an amplifier to a recorder. The number of revolutions and model speed are also recorded.

To avoid sources of error, it is practical to keep the cables from the transmitter to the amplifier as short as possible. This is possible by employing a lightweight amplifier that can be installed into the model. The cable from the amplifier to the recorder is not sensitive, so that its length does not influence the results. The recorder has to be shock-free installed on the carriage. Shocks can cause the measuring loops to oscillate and influence the measurements. Foam-rubber or similar material is a good damping material. The results of the tests are given in Figures 15 through 18. Some definitions should be given before discussing the diagrams. In analogy to the definition of the amplitude ΔM defines the double amplitude of the oscillating torque; that means ΔM is the difference between the

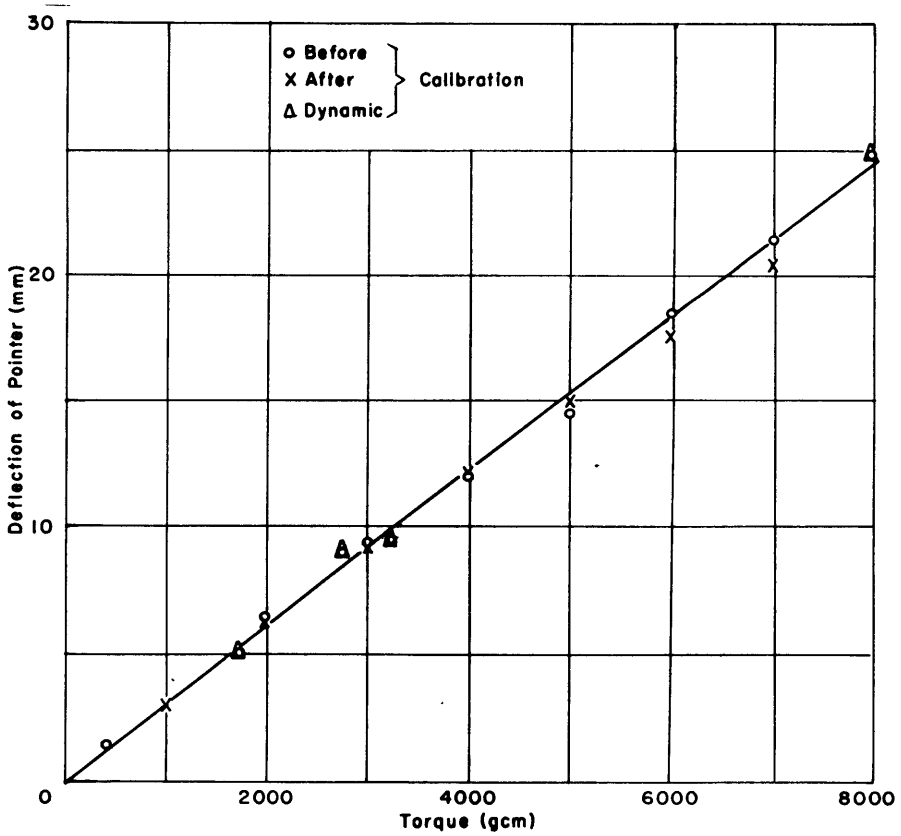

Figure 14

maximum and the minimum of the oscillating torque. $\bar{M}$ denotes the torque necessary to drive the vessel, whereas M_t denotes the oscillating torque as a function of the number of propeller revolutions, the number of blades, and the time. Figure 15 gives the rpm and the magnitude of the oscillating torque (ΔM in gcm) as a function of the model speed for a 3- and 4-bladed propeller. The diagram shows essential characteristics in the behavior of ΔM. The magnitude of ΔM increases with increasing model speed. The ΔM is smaller for a 3-bladed propeller when compared to a 4-bladed propeller at equal speeds, and the 3-bladed propeller has smaller torque oscillation than the 4-bladed propeller. This result is expected when the symmetry of the propeller and the wake field is considered. The scatter of the measuring spots is connected with the control of the model speed. It would be incorrect to draw conclusions from the scatter of the ΔM values to the accuracy of the measuring device.

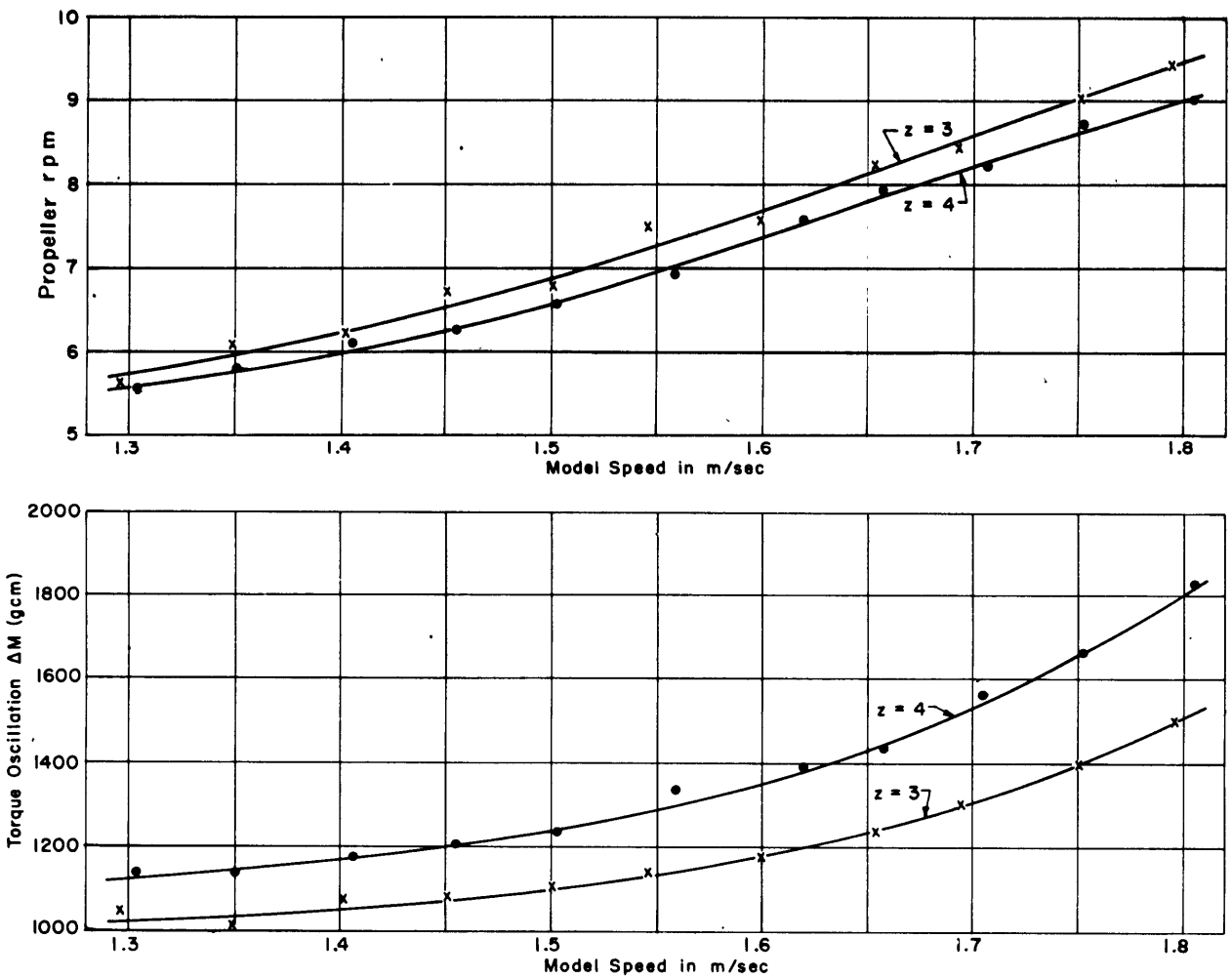

Figure 15

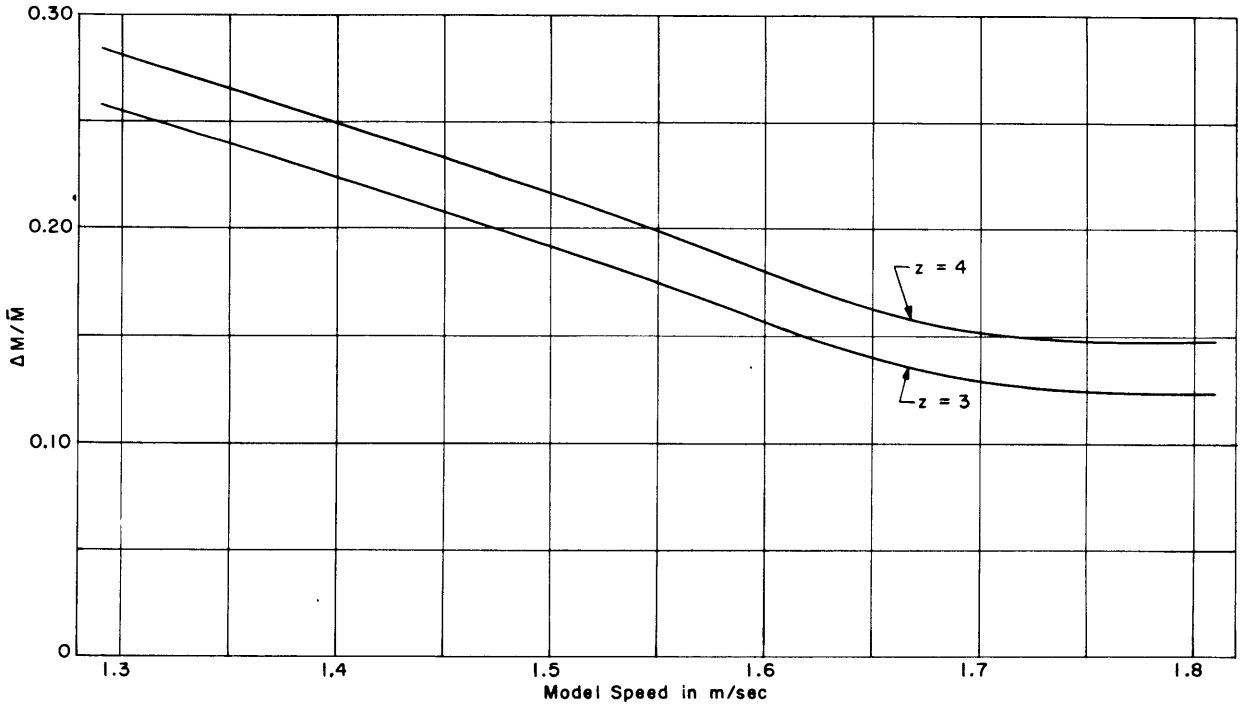

Figure 16

Figure 16 gives the ratio of $\Delta M/\bar{M}$ as a function of the model speed ($\bar{M}$ derived from propulsion tests.) The curves indicate a dropping tendency, which means that the torque $\bar{M}$, necessary to propel the model, increases more than ΔM. The curves have a tendency to become horizontal at speeds above 1.6 m/sec. The model approaches a Froude optimum, which influences, as expected, only $\bar{M}$ and not ΔM. Strong surface effects practically do not influence torque oscillations if the propeller is submerged deep enough.

Furthermore, it is of interest to study the oscillating torque at constant revolutions as a time function. Figure 17 shows the plotting of the 4-bladed propeller and Figure 18 of the 3-bladed propeller. Since oscillation effects occur independently on the zero-line, the zero-line was chosen as the dividing line of the area. A comparison of the two curves clearly indicates a good symmetric course of the torque when considering the 4-bladed propeller within its 1/8 motion (45 deg), whereas there is no symmetry within the 1/6 motion (60 deg) of the 3-bladed propeller. The cause is given by the wake field and the symmetry of the propeller. From the fact that the 4-bladed propeller and the wake have an even symmetry (4 or 2), whereas the 3-bladed propeller has an odd symmetry (3), we may assume that the curves are symmetric or asymetric. The diagrams (Figures 17 and 18) also show the cosine line. The torque and cosine curve agree much better when the 4-bladed propeller is considered. Valuable deductions may be drawn from this statement for theoretical treatment of this problem. As the first step we will consider a Fourier analysis. We will obtain a strongly converging Fourier series as a result of the deviation between the torque and cosine curve for the 4-bladed propeller, that is, only some

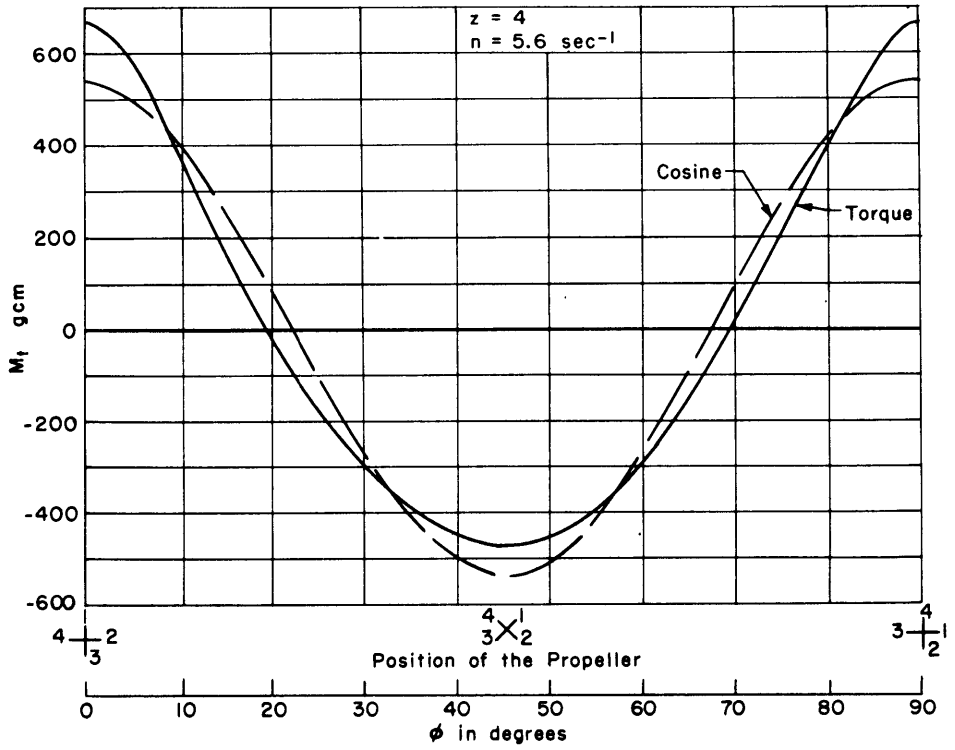

Figure 17

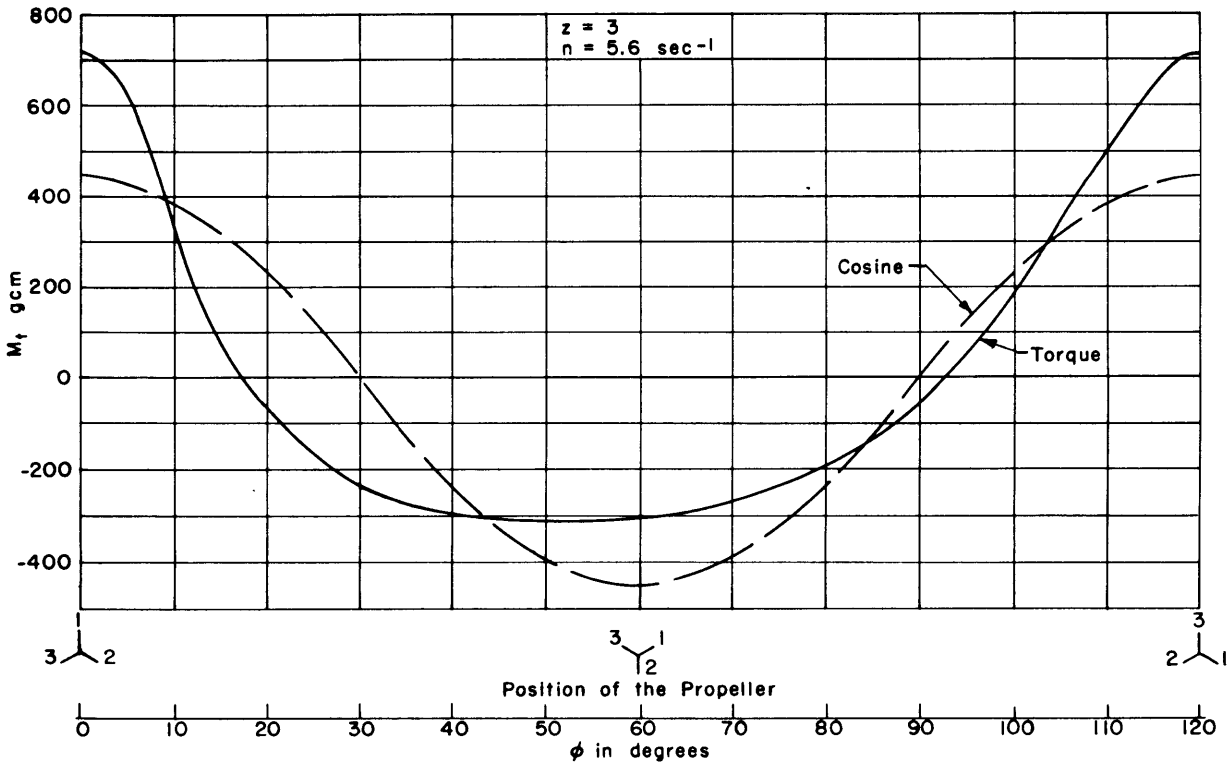

Figure 18

initial members are necessary for a numerical calculation. A quite different situation exists for the 3-bladed propeller. The series converges not so strongly as a result of the large deviation from the cosine line, that is, we have to calculate a very large number of members, which makes the calculation very time-consuming. The question of trying a Fourier integral even arises. This means, physically, that the first harmonics have an influence on the 4-bladed propeller, whereas the higher harmonics are still decisive for the 3-bladed propeller.

To check the accuracy of the results, the device was installed in the model about a week after the tests had been completed. The results showed that the check spots were within the scattering region of the preceding tests. The natural frequency of the instrument amounted to 400 cps.

III. EXPANSION OF THE INSTRUMENTATION TO MEASURE THRUST FLUCTUATIONS

A. INTRODUCTION

A thrust-fluctuation-measuring device was designed so that it could be added to the existing torque oscillation instrument in the form of a measuring head.

The best way to determine thrust fluctuations is by model tests, since the calculation is very difficult because of the many unknown components. This requires the development of a special measuring member analog to the torque-oscillation measurements. Construction difficulties occurred because the instrument required high natural frequencies, independency on friction of the bearings, and installation in an existing device. The thrust fluctuation has to be measured independently from the torque, whereas the thrust members transform the torque. Figure 19 shows the instrument.

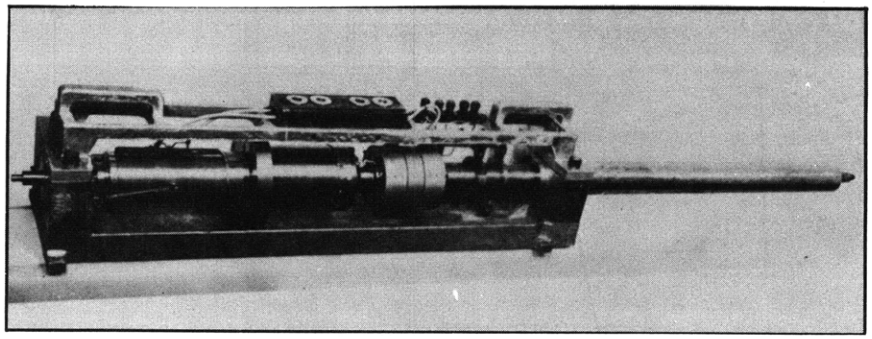

Figure 19

B. DESCRIPTION OF THE DEVICE

The device was so constructed that it could be added to the existing torque-measuring device in the form of a head. By doing so the device becomes independent of bearing influences. Two cylinders, an inner one and an outer one, are connected to one another by a diaphragm ring; see Figure 20. The inner cylinder is connected to the torque shaft, and the outer cylinder supports the propeller. If thrust forces are applied to the propeller, the outer cylinder is displaced in axial direction against the inner one and the membrane ring, mounted normal to the shaft, is deformed; that is, the ring works as a directional spring. The two cylinders and the diaphragm ring are manufactured from one piece of material in order to obtain accurate directional relationship.

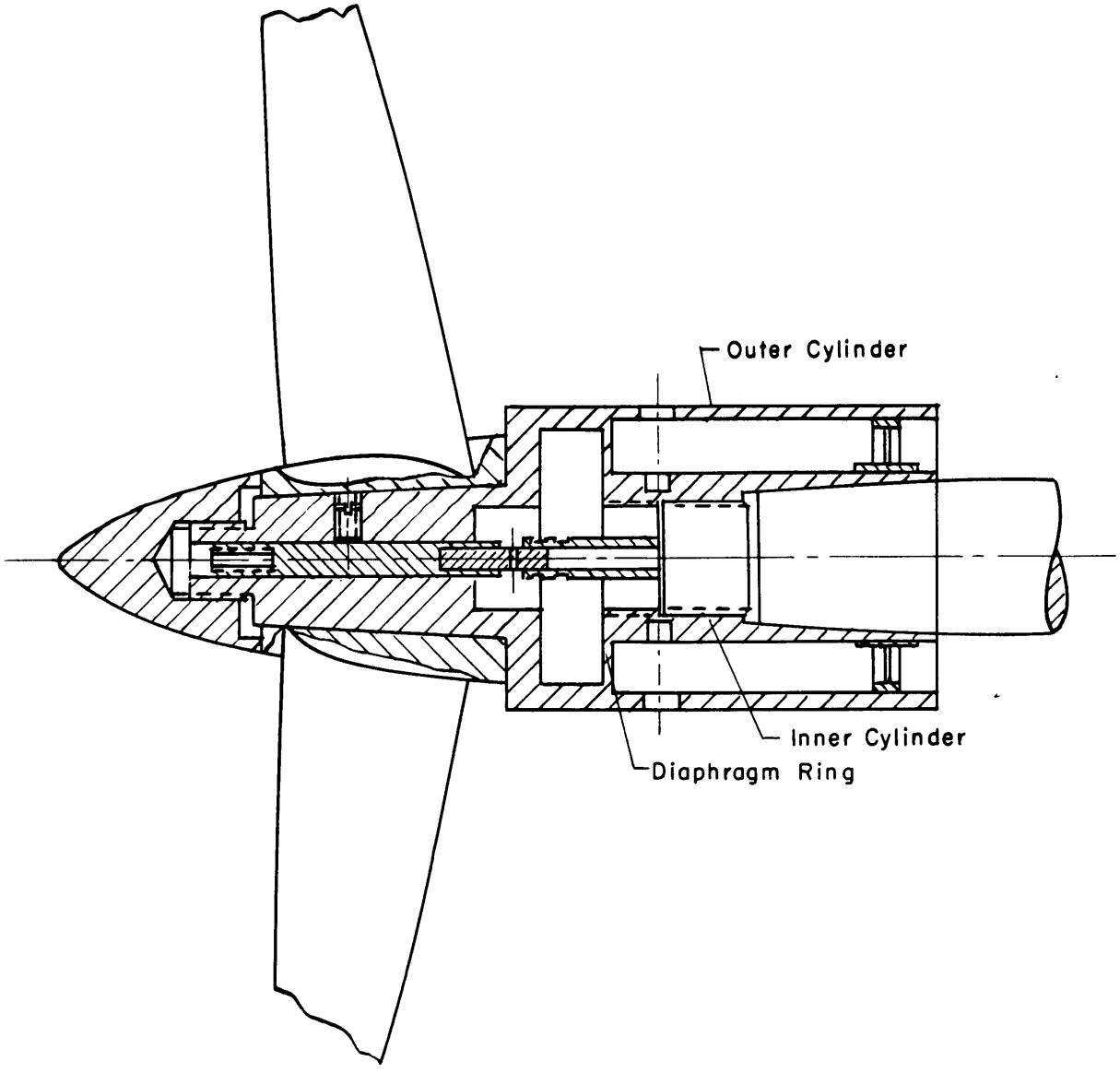

Figure 20

There is a homogeneous connection between the cylinders and the diaphragm ring, which eliminates uncontrollable shifting that often occurs on screw connections. Thus the support conditions are also fixed. This is important because the electrical measuring pickup would be deformed and the transformation of torque would not be accurate. The diaphragm ring works as a directional element but has also the duty to transform the torque. The torque measurement has no influence on the thrust measurements, since a moment-vector, normal to the diaphragm plane, does not move the diaphragm from its original plane. A support ring was designed to prevent the influence of lateral forces and bending moments. This ring is so constructed that it fulfills its task but does not influence the thrust measurements. The natural frequency is above 400 cps as a result of the chosen dimensions of the thrust-measuring head.

An inductive measuring value pickup was chosen to determine the displacement of the two cylinders. This pickup consists of two coils; one is connected to the inner cylinder, the other to the outer cylinder. A shifting of the two cylinders affects the coils and causes a change of the mutual induction of the coils, which means a voltage change takes place.

The measuring principle thus is to transform the shifting of the cylinder (caused by the thrust) into an electrical voltage change and to measure it. It is important that the coils do not contain iron-cores. No hysteresis effect appears; the measuring pickup works linearly. Furthermore, the thrust deforms the diaphragm ring as a result of the small displacement magnitude 10^{-4} mm—according to a linear law. Thus a linear connection exists between the thrust and the voltage change; that is, they are equal with the exception of a constant proportionality factor. The proportionality factor is determined by the calibration of the thrust-measuring member.

The question arose: how to transform the measuring value from the measuring term rotating with the shaft to the amplifier. Since sliprings may influence the measurement and the accuracy may also depend on the rpm, a transformer was installed similar to that used for torque-measurement transfer. The difference consisted in using an inductive method corresponding to the measuring values pickup and not a capacity coupling. This transformer has the advantage that in the case of a small measuring value disturbance, the disturbance is independent of the rpm and thus becomes a constant defined by calibration. The device works as a transformer; one coil rotates with the shaft, the other is at rest.

Figure 21 shows the block diagram of the measuring circuit for thrust and torque oscillations. The parts within the dotted line are the pickups and are one-half the transformer. They rotate with the shaft. The ground connections drawn in the thrust measuring part of the rotating system are not necessarily connected to the resting system by sliprings. The water by which the propeller is supported provides an ideal bridge connection.

C. TESTS AND RESULTS

Two stock models and four stock propellers were chosen to compare the behavior of propellers with different blade numbers behind a model in reference to thrust and torque

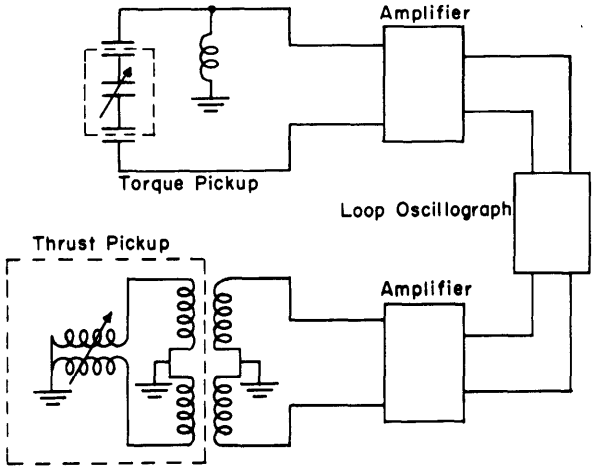

Figure 21

oscillations and to determine the influence of the propeller location within the propeller aperture. The dimensions of the models and the propellers are as follows:

1. Models

L_{BP}	(m)	5.54	6.13
Beam	(m)	0.70	0.89
Draft	(m)	0.328	0.318
Displacement	(kg)	1014	1398
C_B		0.787	0.825

2. Propellers

No. of blades	3	4	5	4
D (mm)	203	203	202.8	200
P (mm)	228	221	215.77	153.5
P/D	1.117	1.09	1.064	0.767
A_e/A	0.484	0.500	0.516	0.540

The torque transmitter and the thrust element were calibrated before the tests started. A calibration factor of 400 gcm/mm deflection was obtained. The calibration curve is given in Figure 22. No deviations occurred in spite of the fact that the calibration extended over several days.

The thrust transmitter was calibrated statically. A thread was connected to the propeller fairing and guided over rolls to be loaded with different weights. The deflections were recorded; see Figure 22. The curve in Figure 22 clearly shows the linear characteristic of the thrust member. The calibration factor is 88 g/mm deflection. A dynamic calibration of the thrust was not performed since a check of the natural frequency showed 400 cps, and

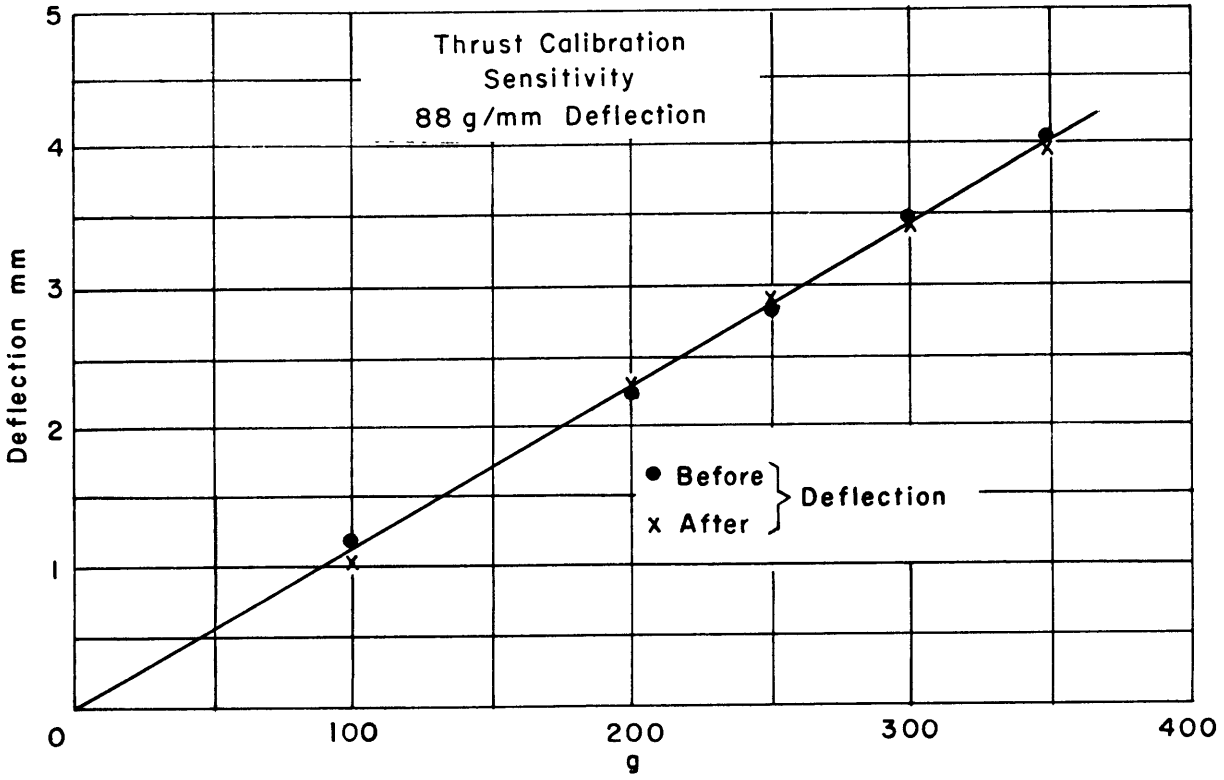
Thrust Calibration
Sensitivity
88 g/mm Deflection
Deflection mm
0
1
2
3
4
5
100
200
300
400
g
● Before
x After
Deflection

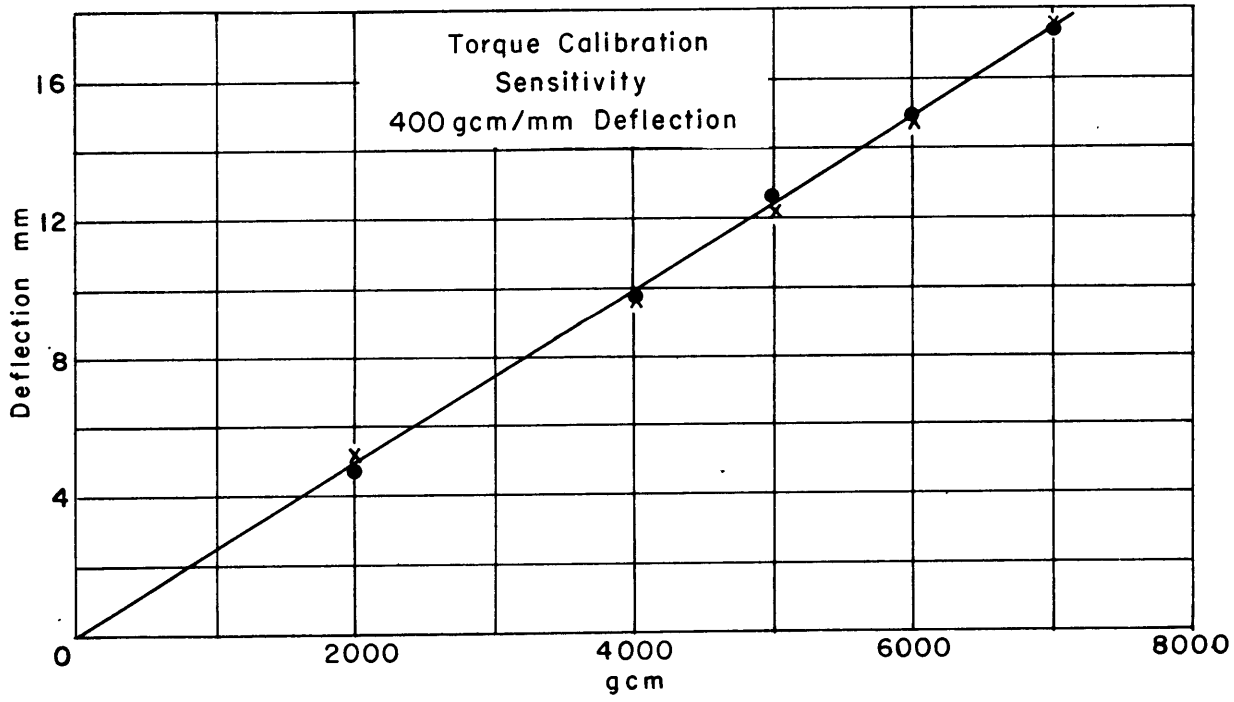
Torque Calibration
Sensitivity
400 gcm/mm Deflection
Deflection mm
0
4
8
12
16
2000
4000
6000
8000
gcm

Figure 22

therefore no differences could be expected between static and dynamic calibrations.

The results given in Figures 23 and 24 indicate that the 4-bladed propeller is the poorest and the 5-bladed propeller the best of the three propellers in reference to thrust and torque oscillations. Lateral forces and bending moments, being in the lines of application within the propeller plane, are missing forces. They appear as alternating bending moments and as alternating forces at the bearing.

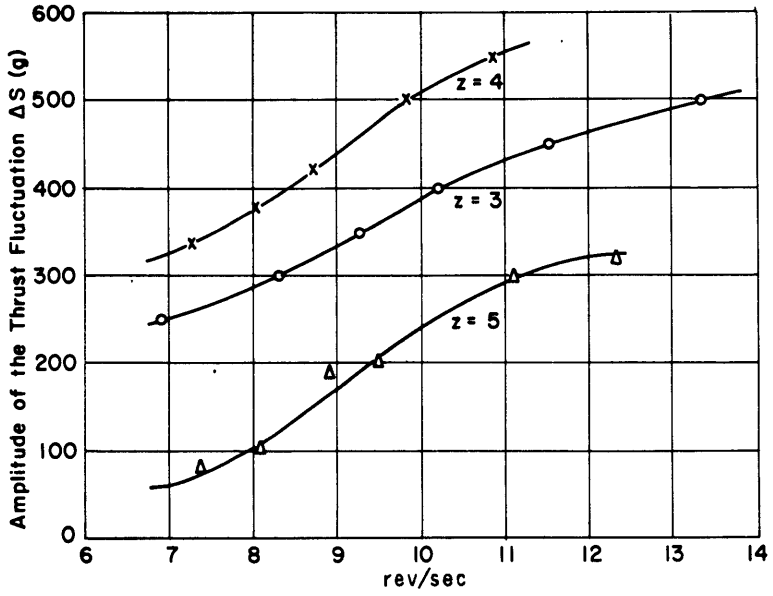

Figure 23

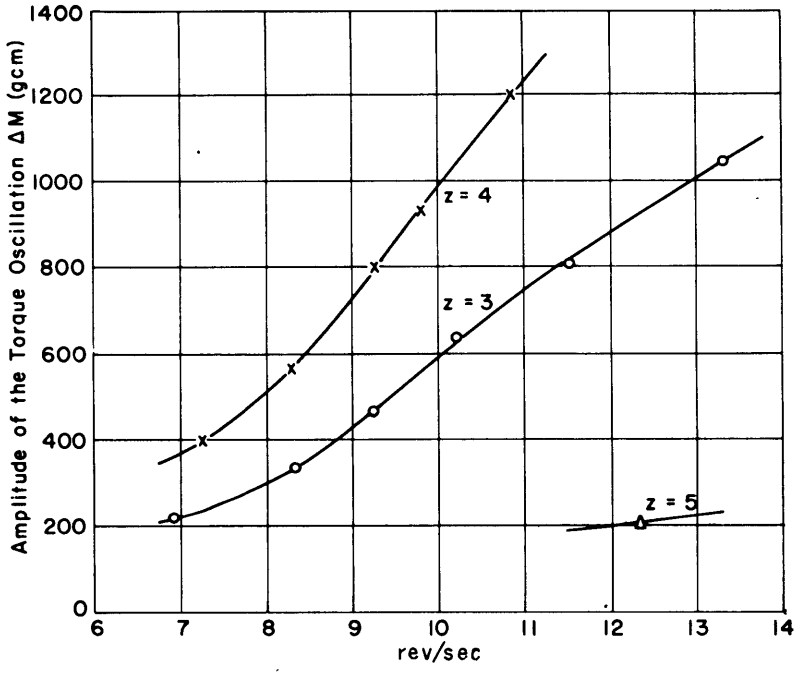

Figure 24

Furthermore, nothing is mentioned about the forces appearing at the hull when the propeller blades pass this region. The choice of a propeller concerning the total oscillating forces depends essentially on the form of the stern and will be different in each case.

The second test series was conducted on a model with a relatively large aperture to shift the propeller a large amount. Furthermore, the deadwood of the stern and the rudder shoe was cut away. The propeller was tested in its normal position, then shifted 30 mm forward and then 30 mm aft. The results are given in Figure 25 (Curves I to III). The corresponding propeller positions are given in Figure 26. The results clearly indicate that the thrust fluctuation decreases with increasing distance from the stern. This shows that it is very important to locate the propeller precisely in the required plane when measuring thrust and torque oscillations.

The influence of a deadwood was also investigated within the test series (see Figure 26, Curve IV), with the propeller located in the normal plane. Curve IV in Figure 25 shows the result, which is comparable with Curve I. The model with the deadwood and the rudder shoe attached increased the oscillations essentially.

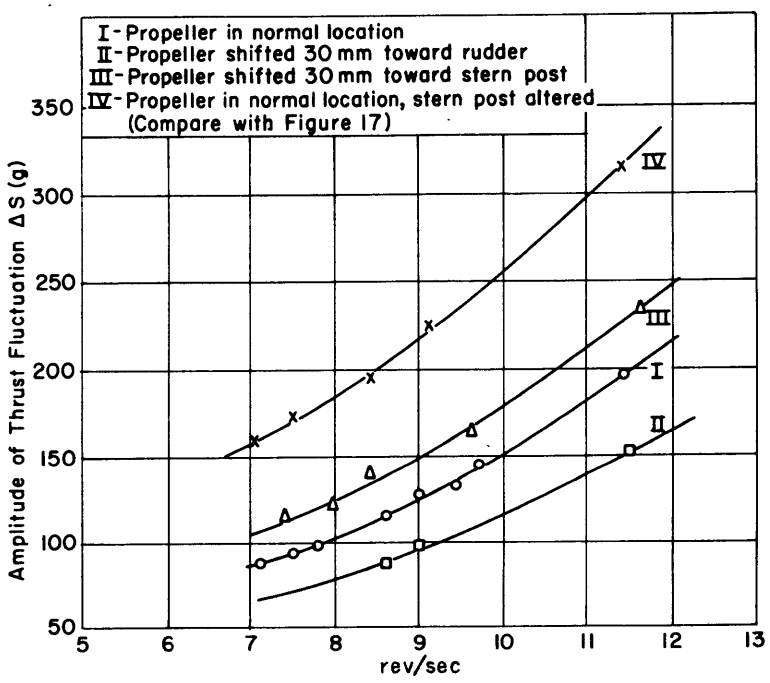

Figure 25

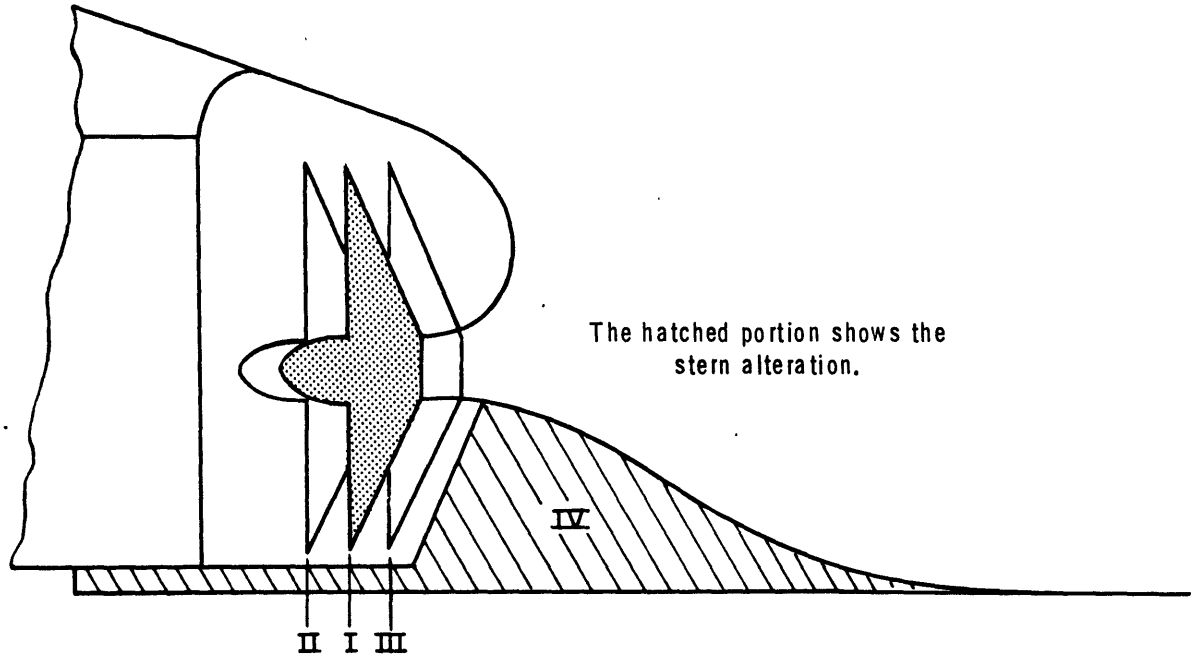

Figure 26

INITIAL DISTRIBUTION

Copies

7 CHBUSHIPS
- 3 Tech Info (Code 335)
- 1 Prelim Des (Code 420)
- 1 Hull Des (Code 440)
- 1 Prop & Shaft (Code 554)
- 1 Ship Noise, Meas, and Red (Code 345)

1 CHONR
- 1 Flu Mech Br (Code 438)

1 DIR, USNRL

1 CDR, USNOL

1 DIR, ORL Penn State

1 ADMIN, U.S. Maritime Adm
Attn: Mr. V.L. Russo

1 Central Tech Dept
Bethlehem Steel Co,
Shipbldg Div, Quincy

1 Engineering Tech Dept
NNS & DD Co

1 Gibbs and Cox, Inc, New York

1 Genl Dyn Corp
Elect Boat Div, Groton

9 SNAME, New York
- 1 Librarian
- 8 H-8 Panel

1 Professor J. Ormondroyd, Univ of Mich

1 Head, Dept NAME, MIT

1 Dept, NAME, Univ of Mich

1 Webb Inst of Nav Arch, Glen Cove

1 DIR, DL, SIT, Hoboken

1 Dept, Nav Arch, Univ of Calif

David Taylor Model Basin. Translation 303.
INVESTIGATIONS OF VIBRATORY FORCES INDUCED BY PROPELLERS (Untersuchungen über die Vibration-serregenden Kräfte am Propeller), by J. Krohn. Translated by W.B. Hinterthan. Feb 1962. ii, 37p. illus., photos., graphs, refs.
UNCLASSIFIED

A method for and the construction of an instrument to measure thrust fluctuations and torque oscillations on a propeller working behind a ship model are given. The propeller shaft is constructed as a hollow shaft in which a second shaft, the measuring shaft, is mounted. The twist of this measuring shaft is transformed by a condenser into an electrical alternating voltage fed by a frequency generator. The modulated alternate voltage is fed into an amplifier connected to a recording instrument. The thrust-measuring instrument is added to the torque-measuring device.

1. Propellers--Thrust--Measurement
2. Propellers--Torque--Measurement
3. Thrust--Measurement--Instrumentation
4. Torque--Measurement--Instrumentation
I. Krohn, J.

David Taylor Model Basin. Translation 303.
INVESTIGATIONS OF VIBRATORY FORCES INDUCED BY PROPELLERS (Untersuchungen über die Vibration-serregenden Kräfte am Propeller), by J. Krohn. Translated by W.B. Hinterthan. Feb 1962. ii, 37p. illus., photos., graphs, refs.
UNCLASSIFIED

A method for and the construction of an instrument to measure thrust fluctuations and torque oscillations on a propeller working behind a ship model are given. The propeller shaft is constructed as a hollow shaft in which a second shaft, the measuring shaft, is mounted. The twist of this measuring shaft is transformed by a condenser into an electrical alternating voltage fed by a frequency generator. The modulated alternate voltage is fed into an amplifier connected to a recording instrument. The thrust-measuring instrument is added to the torque-measuring device.

1. Propellers--Thrust--Measurement
2. Propellers--Torque--Measurement
3. Thrust--Measurement--Instrumentation
4. Torque--Measurement--Instrumentation
I. Krohn, J.

David Taylor Model Basin. Translation 303.
INVESTIGATIONS OF VIBRATORY FORCES INDUCED BY PROPELLERS (Untersuchungen über die Vibration-serregenden Kräfte am Propeller), by J. Krohn. Translated by W.B. Hinterthan. Feb 1962. ii, 37p. illus., photos., graphs, refs.
UNCLASSIFIED

A method for and the construction of an instrument to measure thrust fluctuations and torque oscillations on a propeller working behind a ship model are given. The propeller shaft is constructed as a hollow shaft in which a second shaft, the measuring shaft, is mounted. The twist of this measuring shaft is transformed by a condenser into an electrical alternating voltage fed by a frequency generator. The modulated alternate voltage is fed into an amplifier connected to a recording instrument. The thrust-measuring instrument is added to the torque-measuring device.

1. Propellers--Thrust--Measurement
2. Propellers--Torque--Measurement
3. Thrust--Measurement--Instrumentation
4. Torque--Measurement--Instrumentation
I. Krohn, J.

The deformation of a diaphragm, caused by the thrust, is measured by an inductive pickup system.

Calculations are given to determine the electrical and mechanical dimensions of the instruments. Results of tests conducted with 3-, 4-, and 5-bladed propellers are given.

The deformation of a diaphragm, caused by the thrust, is measured by an inductive pickup system.

Calculations are given to determine the electrical and mechanical dimensions of the instruments. Results of tests conducted with 3-, 4-, and 5-bladed propellers are given.

The deformation of a diaphragm, caused by the thrust, is measured by an inductive pickup system.

Calculations are given to determine the electrical and mechanical dimensions of the instruments. Results of tests conducted with 3-, 4-, and 5-bladed propellers are given.